Chapter 9

Theories of Time Correlation Functions

We turn now to the problem of devising a general theoretical scheme for the calculation of time correlation functions at wavelengths and frequencies on the molecular scale. Memory functions play a key role in the theoretical development and we begin by showing how the memory function approach can be formalised through use of the projection operator methods of Zwanzig[1] and Mori.[2] The calculation of the memory function in a specific problem is a separate task that can be tackled along two different lines. The first represents a systematic extension of the ideas of generalised hydrodynamics introduced in Section 8.6; the second is more microscopic in nature and based on the mode coupling approach already used in Section 8.7.

9.1 THE PROJECTION OPERATOR FORMALISM

Let A be some dynamical variable, dependent in general on the coordinates and momenta of all particles in the system of interest. The definition of A is assumed to be made in such a way that its mean value is zero, but this involves no loss of generality. We have seen in Section 7.1 that if the phase function A is represented by a vector in Liouville space the inner product $(B, A(t))$ of $A(t)$ with the vector representing a second variable B may be identified with the equilibrium time correlation function $C_{AB}(t)$. We can also use a vector in Liouville space to represent a set of dynamical variables of the system, but for the present we restrict ourselves to the single-variable case.

The time variation of the vector $A(t)$ is given by the exact equation of motion (2.1.14). Our aim is to find an alternative to (2.1.14) which is also exact but more easily usable. We proceed by considering the time evolution both of the projection of $A(t)$ onto A (the *projected* part), and of the component of $A(t)$ normal to A (the *orthogonal* part), which we denote by the symbol $A'(t)$. The projection of a second variable $B(t)$ onto A can be written in terms of a linear *projection operator* $\mathcal{P}$ as

$$\mathcal{P}B(t) = \big(A, B(t)\big)(A, A)^{-1}A \tag{9.1.1}$$

Theory of Simple Liquids, Fourth Edition. http://dx.doi.org/10.1016/B978-0-12-387032-2.00009-X

Thus

$$\big(\mathcal{P}B(t), A\big) = \big(A, B(t)\big) \equiv \big\langle B(t)A^*\big\rangle \tag{9.1.2}$$

The complementary operator $\mathcal{Q} = 1 - \mathcal{P}$ projects onto the subspace orthogonal to A. Hence the orthogonal part of $A(t)$ is

$$A'(t) = \mathcal{Q}A(t) \tag{9.1.3}$$

Both $\mathcal{P}$ and $\mathcal{Q}$ satisfy the fundamental properties of projection operators:

$$\mathcal{P}^2 = \mathcal{P}, \quad \mathcal{Q}^2 = \mathcal{Q}, \quad \mathcal{P}\mathcal{Q} = \mathcal{Q}\mathcal{P} = 0 \tag{9.1.4}$$

The projection of $A(t)$ along A is proportional to $Y(t)$, the normalised time autocorrelation function of the variable A, i.e.

$$\mathcal{P}A(t) = Y(t)A \tag{9.1.5}$$

with

$$Y(t) = \big(A, A(t)\big)(A, A)^{-1} \equiv \big\langle A(t)A^*\big\rangle\big\langle AA^*\big\rangle^{-1} = C_{AA}(t)/C_{AA}(0) \tag{9.1.6}$$

The definitions (9.1.1)–(9.1.3) ensure that

$$\big(A, A'(t)\big) = 0 \tag{9.1.7}$$

The first step is to derive an equation for the time evolution of the projected part, $Y(t)$. The Laplace transform of the equation of motion (2.1.14) is

$$(z + \mathcal{L})\tilde{A}(z) \equiv (z + \mathcal{L})(\mathcal{P} + \mathcal{Q})\tilde{A}(z) = iA \tag{9.1.8}$$

Thus

$$\begin{aligned}\tilde{Y}(z) &= \left(A, \int_0^\infty \exp(izt)\exp(i\mathcal{L}t)A\,\mathrm{d}t\right)(A, A)^{-1} \\ &= \big(A, i(z + \mathcal{L})^{-1}A\big)(A, A)^{-1} = \big(A, \tilde{A}(z)\big)(A, A)^{-1}\end{aligned} \tag{9.1.9}$$

where the 'resolvent' operator $i(z + \mathcal{L})^{-1}$ is the transform of the propagator $\exp(i\mathcal{L}t)$. We now project (9.1.8) parallel and perpendicular to A by application, respectively, of the operators $\mathcal{P}$ and $\mathcal{Q}$. Use of the properties (9.1.4) shows that

$$z\mathcal{P}\tilde{A}(z) + \mathcal{P}\mathcal{L}\mathcal{P}\tilde{A}(z) + \mathcal{P}\mathcal{L}\mathcal{Q}\tilde{A}(z) = iA \tag{9.1.10}$$

$$z\mathcal{Q}\tilde{A}(z) + \mathcal{Q}\mathcal{L}\mathcal{P}\tilde{A}(z) + \mathcal{Q}\mathcal{L}\mathcal{Q}\mathcal{Q}\tilde{A}(z) = 0 \tag{9.1.11}$$

and elimination of $\mathcal{Q}\tilde{A}(z)$ between (9.1.10) and (9.1.11) gives

$$z\mathcal{P}\tilde{A}(z) + \mathcal{P}\mathcal{L}\mathcal{P}\tilde{A}(z) - \mathcal{P}\mathcal{L}\mathcal{Q}(z + \mathcal{Q}\mathcal{L}\mathcal{Q})^{-1}\mathcal{Q}\mathcal{L}\mathcal{P}\tilde{A}(z) = iA \tag{9.1.12}$$

If we now take the inner product with A and multiply through by $-i(A,A)^{-1}$, (9.1.12) becomes

$$-iz\tilde{Y}(z) - i\big(A, \mathcal{L}\mathcal{P}\tilde{A}(z)\big)(A,A)^{-1} + i\big(A, \mathcal{L}\mathcal{Q}(z+\mathcal{Q}\mathcal{L}\mathcal{Q})^{-1}\mathcal{Q}\mathcal{L}\mathcal{P}\tilde{A}(z)\big)(A,A)^{-1} = 1 \tag{9.1.13}$$

Since $i\mathcal{L}\mathcal{P}\tilde{A}(z) = (A,A)^{-1}\big(A,\tilde{A}(z)\big)\dot{A}$, this expression can be rewritten as

$$(-iz - i\Omega)\tilde{Y}(z) + \big(K, \tilde{R}(z)\big)(A,A)^{-1}\tilde{Y}(z) = 1 \tag{9.1.14}$$

where

$$K = \mathcal{Q}\dot{A} = \mathcal{Q}(i\mathcal{L})A \tag{9.1.15}$$

is the projection of $\dot{A}$ orthogonal to A and we have introduced the quantity

$$\tilde{R}(z) = i(z+\mathcal{Q}\mathcal{L}\mathcal{Q})^{-1}K \tag{9.1.16}$$

and defined a frequency Ω as

$$i\Omega = (A,\dot{A})(A,A)^{-1} = \dot{Y}(0) \tag{9.1.17}$$

In the single-variable case the frequency Ω is identically zero for systems with continuous interactions, since all autocorrelation functions are even functions of time, but we retain the term in Ω here to facilitate the later generalisation to the multivariable description.

The projection K is conventionally termed a 'random force'. If A is the momentum of particle i, $\dot{A}$ is the total force acting on i and K is then the random force of the classic Langevin theory described in Section 7.3. In other cases, however, K is not a force in the mechanical sense. Instantaneously, K and $\dot{A}$ are the same, but the two quantities evolve differently in time. The time dependence of the random force is given by the inverse Laplace transform of $\tilde{R}(z)$:

$$R(t) = \exp(i\mathcal{Q}\mathcal{L}\mathcal{Q}t)K \tag{9.1.18}$$

with $R(0) = K$. The special form of its propagator means that $R(t)$ remains at all times in the subspace orthogonal to A, i.e.

$$\big(A, R(t)\big) = 0 \quad \text{for all } t \tag{9.1.19}$$

This is easily proved by expanding the right-hand side of (9.1.18) in powers of t, since it is clear by inspection that every term in the series is orthogonal to A. The expansion also reveals that the propagator in (9.1.18) may equally well be written as $\exp(i\mathcal{Q}\mathcal{L}t)$ and both forms appear in the literature. The autocorrelation function of the random force defines the memory function $M(t)$ for the evolution of the dynamical variable A:

$$M(t) = \big(R, R(t)\big)(A,A)^{-1} \tag{9.1.20}$$

or

$$\tilde{M}(z) = \big(R, \tilde{R}(z)\big)(A, A)^{-1} \tag{9.1.21}$$

Equation (9.1.14) can be rewritten in terms of the memory function as

$$\tilde{Y}(z) = \big[-iz - i\Omega + \tilde{M}(z)\big]^{-1} \tag{9.1.22}$$

or, in the time domain, as

$$\dot{Y}(t) - i\Omega Y(t) + \int_0^t M(t-s)Y(s)\mathrm{d}s = 0 \tag{9.1.23}$$

The equation describing the time evolution of the orthogonal component $A'(t)$ is obtained along similar lines. From (9.1.11) we find that for $\tilde{A}'(z) = \mathcal{Q}\tilde{A}(z)$:

$$\begin{aligned}(z + \mathcal{Q}\mathcal{L}\mathcal{Q})\tilde{A}'(z) &= -\mathcal{Q}\mathcal{L}\mathcal{P}\tilde{A}(z) \\ &= -\mathcal{Q}\mathcal{L}\tilde{Y}(z)A = i\tilde{Y}(z)K\end{aligned} \tag{9.1.24}$$

If we substitute for $\tilde{Y}(z)$ from (9.1.22) and use the definition of $\tilde{R}(z)$ in (9.1.16), (9.1.24) becomes

$$\tilde{R}(z) = \big[-iz - i\Omega + \tilde{M}(z)\big]\tilde{A}'(z) \tag{9.1.25}$$

or, in the time domain:

$$\dot{A}'(t) - i\Omega A'(t) + \int_0^t M(t-s)A'(s)\mathrm{d}s = R(t) \tag{9.1.26}$$

Equations (9.1.23) and (9.1.26) are the projections parallel and perpendicular to the variable A of a generalised Langevin equation for A:

$$\dot{A}(t) - i\Omega A(t) + \int_0^t M(t-s)A(s)\mathrm{d}s = R(t) \tag{9.1.27}$$

Apart from the introduction of the term in Ω, (9.1.27) has the same general form as the Langevin equation (7.3.21), but the random force $R(t)$ and memory function $M(t)$ now have the explicit definitions provided by (9.1.18) and (9.1.20).

There is a close connection between the behaviour of the functions $Y(t)$ and $M(t)$ at short times, a fact already exploited in Section 7.3. When differentiated with respect to time the memory function equation (9.1.23) becomes

$$\ddot{Y}(t) - i\Omega\dot{Y}(t) + M(0)Y(t) + \int_0^t \dot{M}(t-s)Y(s)\mathrm{d}s = 0 \tag{9.1.28}$$

Since $Y(0) = 1$ and $\dot{Y}(0) = i\Omega$, we see that

$$M(0) = -\ddot{Y}(0) - \Omega^2 = (\dot{A}, \dot{A})(A, A)^{-1} - \Omega^2 \tag{9.1.29}$$

Repeated differentiation leads to relations between the initial time derivatives of $Y(t)$ and $M(t)$ or, equivalently, given (7.1.24), between the frequency moments of the power spectra $Y(\omega)$ and $M(\omega)$. These relations are useful in constructing

simple, approximate forms for $M(t)$ that satisfy the low-order sum rules on $Y(t)$. A link also exists between the autocorrelation function of the random force, i.e. the memory function, and that of the total force, $\dot{A}$. Let $\Phi(t)$ be the autocorrelation function of $\dot{A}$, defined as

$$\Phi(t) = \big(\dot{A}, \dot{A}(t)\big)(A, A)^{-1} = -\ddot{Y}(t) \tag{9.1.30}$$

It follows from the properties of the Laplace transform that the functions $\tilde{\Phi}(z)$ and $\tilde{Y}(z)$ are related by

$$\tilde{\Phi}(z) = z^2\tilde{Y}(z) - iz + i\Omega \tag{9.1.31}$$

Since the term $i\Omega$ vanishes in the one-variable case, we may temporarily discard it. Then elimination of $\tilde{Y}(z)$ between (9.1.22) and (9.1.31) leads to the expression

$$\frac{1}{\tilde{M}(z)} = \frac{1}{\tilde{\Phi}(z)} + \frac{1}{iz} \tag{9.1.32}$$

The two autocorrelation functions therefore vary with time in different ways except in the high-frequency (short-time) limit: the time dependence of $\Phi(t)$ is determined by the full Liouville operator $\mathcal{L}$ and that of $M(t)$ by the projected operator $\mathcal{Q}\mathcal{L}\mathcal{Q}$.

There are two important ways in which the projection operator formalism can be extended. First, (9.1.23) may be regarded as the the leading member in a hierarchy of memory function equations. If we apply the methods already used to the case when R is treated as the dynamical variable, we obtain an equation similar to (9.1.23) for the time evolution of the projection of $R(t)$ along R. The kernel of the integral equation is now the autocorrelation function of a second-order random force which is orthogonal at all times to both R and A. As an obvious generalisation of this procedure we can write a memory function equation of the form

$$\dot{M}_n(t) - i\Omega_n M_n(t) + \int_0^t M_{n+1}(t-s)\Delta_{n+1}^2 M_n(s)\mathrm{d}s = 0 \tag{9.1.33}$$

where

$$\begin{aligned} M_n(t) &= \big(R_n, R_n(t)\big)(R_n, R_n)^{-1} \\ R_n(t) &= \exp\left(i\mathcal{Q}_n\mathcal{L}\mathcal{Q}_n t\right)\mathcal{Q}_n\dot{R}_{n-1} \end{aligned} \tag{9.1.34}$$

and

$$\Delta_n^2 = (R_n, R_n)(R_{n-1}, R_{n-1})^{-1} \tag{9.1.35}$$

The operator $\mathcal{P}_n$ projects a dynamical variable along R_{n-1} according to the rule (9.1.1). By construction, therefore, the complementary operator

$$\mathcal{Q}_n = 1 - \sum_{j=1}^{n} \mathcal{P}_j \tag{9.1.36}$$

projects onto the subspace orthogonal to all R_j for $j < n$. Thus the nth-order random force $R_n(t)$ is uncorrelated at all times with random forces of

lower order. Equation (9.1.23) is a special case of (9.1.33) with $Y \equiv M_0$. Repeated application of the Laplace transform to equations of the hierarchy leads to an expression for $\tilde{Y}(z)$ in the form of a continued fraction:

$$\tilde{Y}(z) = \cfrac{1}{-iz - i\Omega_0 + \cfrac{\Delta_1^2}{-iz - i\Omega_1 + \cfrac{\Delta_2^2}{-iz - i\Omega_2 + \cdots}}} \tag{9.1.37}$$

A second extension of the method, which has proved particularly useful for the description of collective modes in liquids, is one already mentioned. This is the generalisation to the case where the dynamical quantity of interest is not a single fluctuating property of the system but a set of n independent variables $A_1, A_2, \ldots, A_n$. We represent this set by a column vector $\mathbf{A}$ and its hermitian conjugate by the row vector $\mathbf{A}^*$. The derivation of the generalised Langevin equation for $\mathbf{A}$ follows the lines already laid down, due account being taken of the fact that the quantities involved are no longer scalars. The result may be written in matrix form as

$$\dot{\mathbf{A}}(t) - i\boldsymbol{\Omega} \cdot \mathbf{A}(t) + \int_0^t \mathbf{M}(t-s) \cdot \mathbf{A}(s)\mathrm{d}s = \mathbf{R}(t) \tag{9.1.38}$$

The definitions of the random force vector $\mathbf{R}(t)$, frequency matrix $\boldsymbol{\Omega}$ and memory function matrix $\mathbf{M}(t)$ are analogous to those of $R(t), \Omega$ and $M(t)$ in the single-variable case, the scalars A and A^* being replaced by the vectors $\mathbf{A}$ and $\mathbf{A}^*$. If we multiply (9.1.38) from the right by $\mathbf{A}^* \cdot (\mathbf{A}, \mathbf{A})^{-1}$ and take the thermal average we find that

$$\dot{\mathbf{Y}}(t) - i\boldsymbol{\Omega}\dot{\mathbf{Y}}(t) + \int_0^t \mathbf{M}(t-s) \cdot \mathbf{Y}(s)\mathrm{d}s = \mathbf{0} \tag{9.1.39}$$

where $\mathbf{Y}(t) = (\mathbf{A}, \mathbf{A}(t)) \cdot (\mathbf{A}, \mathbf{A})^{-1}$ is the correlation function matrix. Equation (9.1.39) is the multi-variable generalisation of (9.1.23); its solution in terms of Laplace transforms is

$$\tilde{\mathbf{Y}}(z) = [-iz\,\mathbf{I} - i\boldsymbol{\Omega} + \tilde{\mathbf{M}}(z)]^{-1} \tag{9.1.40}$$

where $\mathbf{I}$ is the identity matrix. Note that each diagonal element of $\mathbf{Y}(t)$ is an autocorrelation function, normalised by its value at $t = 0$, and the off-diagonal elements are cross-correlation functions.

The value of the memory function formalism is most easily appreciated by considering specific examples of its use. Before doing so, however, it is helpful to look at the problem from a wider point of view. Equation (9.1.38) represents an equation of motion for $\mathbf{A}(t)$ in which terms linear in $\mathbf{A}$ are displayed explicitly on the left-hand side while the random force vector describes the effects of non-linear terms, initial transient processes and the dependence of $\mathbf{A}(t)$ on variables not included in the set $\{A_i\}$. This separation of effects is most useful in cases where the random force fluctuates rapidly and the non-zero

elements of the memory function matrix decay much faster than the correlation functions of interest. It is then not unreasonable to represent $\mathbf{M}(t)$ in some simple way, in particular by invoking a Markovian approximation whereby the non-zero elements are replaced by δ-functions in t. For this representation to be successful the vector $\mathbf{A}$ should contain as its components not only the variables of immediate interest but also those to which they are strongly coupled. If the set of variables is well chosen the effect of projecting $\mathbf{A}(t)$ onto the subspace spanned by $\mathbf{A}$ is to project out all the slowly varying properties of the system. The Markovian assumption can then be used with greater confidence in approximating the memory function matrix. By extending the dimensionality of $\mathbf{A}$ an increasingly detailed description can be obtained without departing from the Markovian hypothesis. In practice, as we shall see in later sections, this ideal state of affairs is often difficult to achieve, and some of the elements of $\mathbf{M}(t)$ may not be truly short ranged in time. The calculation of the frequency matrix $\boldsymbol{\Omega}$ is usually a straightforward problem, since it involves only static quantities; the same is true of the static correlation matrix $(\mathbf{A}, \mathbf{A})$.

As an alternative to the multi-dimensional description it is possible to work with a smaller set of variables and exploit the continued-fraction expansion, truncating the hierarchy at a suitable point in some simple, approximate way. This approach is particularly useful when insufficient is known about the dynamical behaviour of the system to permit an informed choice of a larger set of variables. Its main disadvantage is the fact that the physical significance of the memory function becomes increasingly obscure as the expansion is carried to higher orders.

9.2 SELF CORRELATION FUNCTIONS

As a simple example we consider first the application of projection operator methods to the calculation of the self-intermediate scattering function $F_s(k,t)$. This function is of interest because of its link to the velocity autocorrelation function via (8.2.17) and because its power spectrum, the self dynamic structure factor $S_s(k,\omega)$, is closely related to the cross-section for incoherent scattering of neutrons.

The most straightforward approach to the problem is to choose as the single variable A the fluctuating density $\rho_{\mathbf{k}i}$ of a tagged particle i and write a memory function equation for $\tilde{F}_s(k,z)$ in the form

$$\tilde{F}_s(k,z) = \frac{1}{-iz + \tilde{M}_s(k,z)} \tag{9.2.1}$$

Results given in Section 8.2 show that the short-time expansion of $F_s(k,t)$ starts as

$$F_s(k,t) = 1 - \omega_0^2 \frac{t^2}{2!} + \omega_0^2(3\omega_0^2 + \Omega_0^2)\frac{t^4}{4!} + \cdots \tag{9.2.2}$$

where the coefficients of successive powers of t are related to the frequency moments of $S_s(k,\omega)$ via the general expression (7.1.24) and the quantities Ω_0 (the Einstein frequency) and ω_0 are defined by (7.2.9) and (7.4.29) respectively; it follows from (9.1.29) that the effect of setting $M_s(k,t=0) = \omega_0^2 = k^2(k_B T/m)$ is to ensure that $S_s(k,\omega)$ has the correct second moment. We may also rewrite $\tilde{M}_s(k,z)$ as $k^2\tilde{D}(k,z)$ where, by analogy with (8.2.10), $\tilde{D}(k,z)$ plays the role of a generalised self-diffusion coefficient such that $\lim_{z\to 0}\lim_{k\to 0}\tilde{D}(k,z) = D$. If the continued-fraction expansion is taken to second order we find that

$$\tilde{F}_s(k,z) = \cfrac{1}{-iz + \cfrac{\omega_0^2}{-iz + \tilde{N}_s(k,z)}} \tag{9.2.3}$$

By extension of the calculation that leads to (9.1.29) it is easy to show that the initial value of the second-order memory function $N_s(k,t)$ is related to the short-time behaviour of $M_s(k,t)$ by $N_s(k,0) = -\ddot{M}_s(k,0)/M_s(k,0) = 2\omega_0^2 + \Omega_0^2$. Thus, if

$$\tilde{N}_s(k,z) = \left(2\omega_0^2 + \Omega_0^2\right)\tilde{n}_s(k,z) \tag{9.2.4}$$

where $n_s(k,t=0)=1$, the resulting expression for $S_s(k,\omega)$ also has the correct fourth moment regardless of the time dependence of $n_s(k,t)$.

As an alternative to making a continued-fraction expansion of $\tilde{F}_s(k,z)$ we can consider the multi-variable description of the problem that comes from the choice

$$\mathbf{A} = \begin{pmatrix} \rho_{\mathbf{k}i} \\ \dot{\rho}_{\mathbf{k}i} \\ \sigma_{\mathbf{k}i} \end{pmatrix} \tag{9.2.5}$$

where the variable $\sigma_{\mathbf{k}i}$, given by

$$\sigma_{\mathbf{k}i} = \ddot{\rho}_{\mathbf{k}i} - (\rho_{\mathbf{k}i}, \ddot{\rho}_{\mathbf{k}i})(\rho_{\mathbf{k}i}, \rho_{\mathbf{k}i})^{-1}\rho_{\mathbf{k}i} \tag{9.2.6}$$

is orthogonal to both $\rho_{\mathbf{k}i}$ and $\dot{\rho}_{\mathbf{k}i}$. From results derived in Sections 7.4 and 8.2 it is straightforward to show that the corresponding static correlation matrix is diagonal and given by

$$(\mathbf{A},\mathbf{A}) = \begin{pmatrix} 1 & 0 & 0 \\ 0 & \omega_0^2 & 0 \\ 0 & 0 & \omega_0^2(2\omega_0^2 + \Omega_0^2) \end{pmatrix} \tag{9.2.7}$$

while the frequency matrix is purely off-diagonal:

$$i\boldsymbol{\Omega} = (\mathbf{A},\dot{\mathbf{A}})\cdot(\mathbf{A},\mathbf{A})^{-1} = \begin{pmatrix} 0 & 1 & 0 \\ -\omega_0^2 & 0 & 1 \\ 0 & -2\omega_0^2 - \Omega_0^2 & 0 \end{pmatrix} \tag{9.2.8}$$

Both $\dot{A}_1$ and $\dot{A}_2$ form part of the space spanned by the vector $\mathbf{A}$. In the case of $\dot{A}_1$ this is easy to see, since $\dot{A}_1 = A_2$. To understand why it is is also true for $\dot{A}_2$ it is sufficient to note that the projection of $\dot{A}_2$ along A_1 is obviously part of the space of $\mathbf{A}$, whereas the component orthogonal to A_1 is, according to the definition (9.2.6), the same as A_3. It follows that the random-force vector has only one non-zero component and the memory function matrix has only one non-zero entry:

$$\mathbf{M}(k,t) = \begin{pmatrix} 0 & 0 & 0 \\ 0 & 0 & 0 \\ 0 & 0 & \mathcal{M}(k,t) \end{pmatrix} \tag{9.2.9}$$

On collecting results and inserting them in (9.1.40), we find that the correlation function matrix has the form

$$\tilde{\mathbf{Y}}(k,z) = \begin{pmatrix} -iz & -1 & 0 \\ \omega_0^2 & -iz & -1 \\ 0 & 2\omega_0^2 + \Omega_0^2 & -iz + \tilde{\mathcal{M}}(k,z) \end{pmatrix}^{-1} \tag{9.2.10}$$

Inversion of (9.2.10) shows that $\tilde{F}_s(k,z)$ is given by

$$\begin{aligned} \tilde{F}_s(k,z) &= \tilde{Y}_{11}(k,z) \\ &= \cfrac{1}{-iz + \cfrac{\omega_0^2}{-iz + \cfrac{2\omega_0^2 + \Omega_0^2}{-iz + \tilde{\mathcal{M}}(k,z)}}} \end{aligned} \tag{9.2.11}$$

and comparison with (9.2.3) and (9.2.4) makes it possible to identify $\mathcal{M}(k,t)$ as the memory function of $N_s(k,t)$. Similarly, the Laplace transform of the self current autocorrelation function $C_s(k,t)$ is

$$\begin{aligned} \tilde{C}_s(k,z) &= \omega_0^2 \tilde{Y}_{22}(k,z) \\ &= \cfrac{\omega_0^2}{-iz + (2\omega_0^2 + \Omega_0^2)\tilde{n}_s(k,z) + \cfrac{\omega_0^2}{-iz}} \end{aligned} \tag{9.2.12}$$

The same result can be derived from (9.2.3) via the relation (8.2.17) between $C_s(k,t)$ and $F_s(k,t)$, which in turn implies that $\tilde{C}_s(k,z) = z^2\tilde{F}_s(k,z) - iz$.

In the long-wavelength limit the memory function $n_s(k,t)$ is directly related to the memory function of the velocity autocorrelation function $Z(t)$. From (7.2.8), (8.2.17) and (9.2.12) we find that

$$\tilde{Z}(z) = \frac{k_B T/m}{-iz + \Omega_0^2 \tilde{n}_s(0,z)} \tag{9.2.13}$$

Thus

$$N_s(0,t) = \Omega_0^2 n_s(0,t) \equiv \xi(t) \tag{9.2.14}$$

where $\xi(t)$ is the memory function of $Z(t)$, introduced earlier in Section 7.3. Since $N_s(k,t)$ is also the memory function of $M_s(k,t)$ and $M_s(k,0) = k^2 Z(0)$, we see that $k^2 Z(t)$ becomes the memory function of $F_s(k,t)$ as $k \to 0$. For consistency with the hydrodynamic result (8.2.10) we also require that

$$\Omega_0^2 \tilde{n}_s(0,0) = \frac{k_B T}{mD} \tag{9.2.15}$$

A particularly simple (Markovian) approximation is to replace $N_s(k,t)$ by a quantity independent of t, $1/\tau_s(k)$ say, which is equivalent to assuming an exponential form for $M_s(k,t)$:

$$M_s(k,t) = \omega_0^2 \exp\big[-|t|/\tau_s(k)\big] \tag{9.2.16}$$

with the constraint, required to satisfy (9.2.15), that

$$\tau_s(0) = \frac{mD}{k_B T} \tag{9.2.17}$$

As we have seen in Section 7.3, this approximation leads to an exponential velocity autocorrelation function of the Langevin type, the quantity $1/\tau_s(0)$ appearing as a frequency independent friction coefficient. Better results are obtained by choosing an exponential form for $N_s(k,t)$, i.e.

$$N_s(k,t) = \big(2\omega_0^2 + \Omega_0^2\big) \exp\big[-|t|/\tau_s(k)\big] \tag{9.2.18}$$

with

$$\tau_s(0) = \frac{k_B T}{mD\Omega_0^2} \tag{9.2.19}$$

This second approximation is equivalent to neglecting the frequency dependence of $\tilde{\mathcal{M}}(k,z)$; it leads to an analytical form for $S_s(k,\omega)$ having the correct zeroth, second and fourth moments:

$$S_s(k,\omega) = \frac{1}{\pi} \frac{\tau_s(k)\omega_0^2(2\omega_0^2 + \Omega_0^2)}{\omega^2\tau_s^2(k)(\omega^2 - 3\omega_0^2 - \Omega_0^2)^2 + (\omega^2 - \omega_0^2)^2} \tag{9.2.20}$$

The corresponding expression for $\tilde{Z}(z)$ is that given in (7.3.26), with $\tau \equiv \tau_s(0)$.

In the absence of any well-based microscopic theory it is perhaps best to treat the relaxation time $\tau_s(k)$ as an adjustable parameter, but it is also tempting to look for some relatively simple prescription for this quantity. An argument based on a scaling of the memory function $M_s(k,t)$ has been used to derive the expression[3]

$$\tau_s^{-1}(k) = \gamma(2\omega_0^2 + \Omega_0^2)^{1/2} \tag{9.2.21}$$

where the parameter γ is taken to be independent of k, an assumption which is reasonably well-borne out in practice. If, in the limit $k \to 0$, we require (9.2.21) to yield the correct diffusion coefficient, it follows that $\gamma = mD\Omega_0/k_B T$; this leads to a value of γ of $\approx$0.9 at the triple point of liquid argon. On the other hand, for large wavenumbers, $S_s(k, 0)$ goes over correctly to the ideal gas result if $\gamma = 2/\pi^{1/2} \approx 1.13$.

Although the exponential approximation (9.2.18) has been used with some success in the interpretation of experimental neutron scattering data,[4] the true situation is known to be much less simple, at least at small wavenumbers. In particular, molecular dynamics calculations for a range of simple liquids have shown that the memory function of $Z(t)$, i.e. $N_s(0, t)$, cannot be adequately described by a model involving only a single relaxation time. Figure 9.1 shows the memory function obtained from a simulation of liquid sodium[5] in which a clear separation of time scales is apparent; the presence of the long-time tail in the memory function has the effect of reducing the self-diffusion coefficient by about 30%. In their analysis of the self-correlation functions of the Lennard-Jones fluid Levesque and Verlet[6] found it necessary to use a rather complicated expression for $N_s(k, t)$, which for $k = 0$ reduces to

$$\xi(t) = \Omega_0^2 \exp\left[-(t/\tau_1)^2\right] + At^4 \exp\left(-t/\tau_2\right) \tag{9.2.22}$$

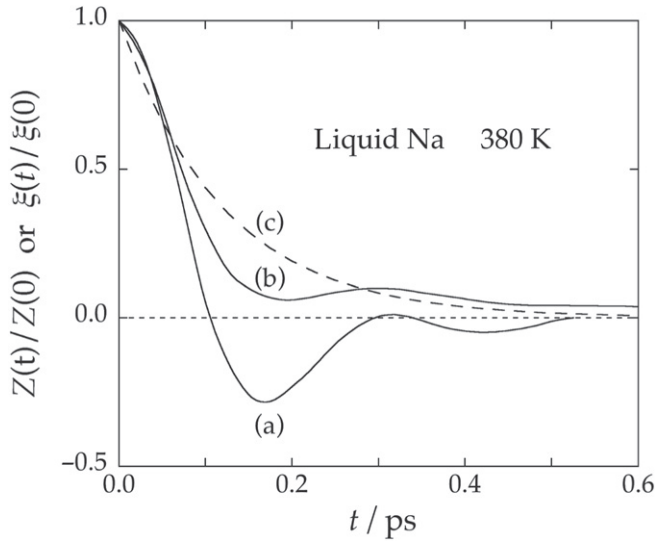

FIGURE 9.1 Velocity autocorrelation function, curve (a), and the associated memory function, curve (b), derived from molecular dynamics calculations for liquid sodium at state conditions close to the normal melting point. Curve (c) shows the exponential approximation (9.2.18) for the memory function, with $\tau_s(0)$ chosen to give the correct self-diffusion coefficient. From U. Balucani et al., *J. Non-Cryst. Solids* **205–207**, 299–303 (1996),*with permission of Elsevier.*

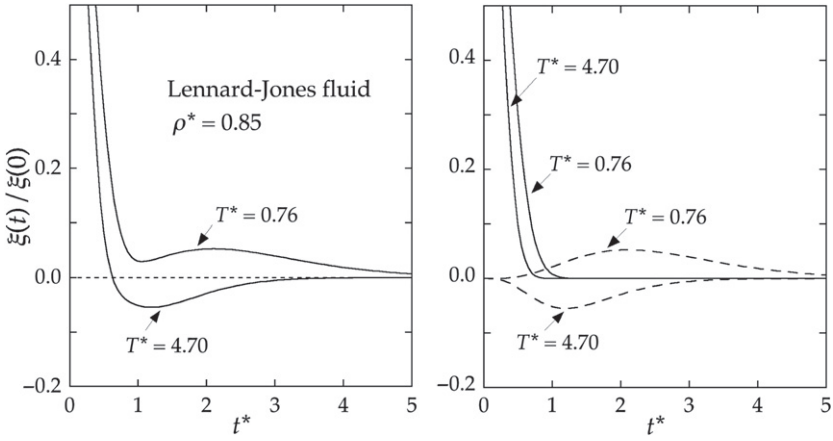

FIGURE 9.2 Normalised memory function associated with the velocity autocorrelation function of the Lennard-Jones fluid at a density $\rho^* = 0.85$ and two temperatures. Left-hand panel: the total memory function. Right-hand panel: the decomposition into short-lived (full curves) and long-lived (dashed curves) components, corresponding to the two terms in (9.2.22). After Levesque and Verlet.[6]

where A, τ_1 and τ_2 are adjustable parameters. A separation into a rapidly decaying part and a long-lived term that starts as t^4 is also an explicit ingredient of modern versions of kinetic theory, in which account is taken of correlated as well as uncorrelated collisions. The long-lived term represents collective effects and lends itself to calculation by mode coupling methods similar to that employed in Section 8.7, which we shall meet again later in this chapter. The relaxation time τ_1 decreases with temperature but is almost independent of density while τ_2 increases with density but is insensitive to changes in temperature. The behaviour of the parameter A is more complicated. Figure 9.2 shows the memory function at a high density and two temperatures. At the lower value of T^* the contribution from the long-lived term is positive and the memory function is very similar in form to that for liquid sodium pictured in Figure 9.1. As the temperature is raised – or the density lowered – A decreases in magnitude and eventually changes sign. This gives rise to a negative region in the memory function, which is the source of a persisting positive correlation of velocity of the type seen, for example, in Figure 7.1 for the case of the r^{-12}-fluid at a low value of the coupling parameter Γ.

The importance of including a long-lived component in the memory function $N_s(k,t)$ for $k > 0$ is illustrated for the case of the Lennard-Jones fluid close to the triple point in Figure 9.3. The quantity plotted there, as a function of k, is the width at half-height of $S_s(k,\omega)$ relative to its value in the hydrodynamic limit (where $\Delta\omega = 2Dk^2$). Comparison with results for $S_s(k\omega)$ itself is not very illuminating, since the spectrum is largely featureless, but the dependence of $\Delta\omega/Dk^2$ on k displays a structure that is very poorly described by the

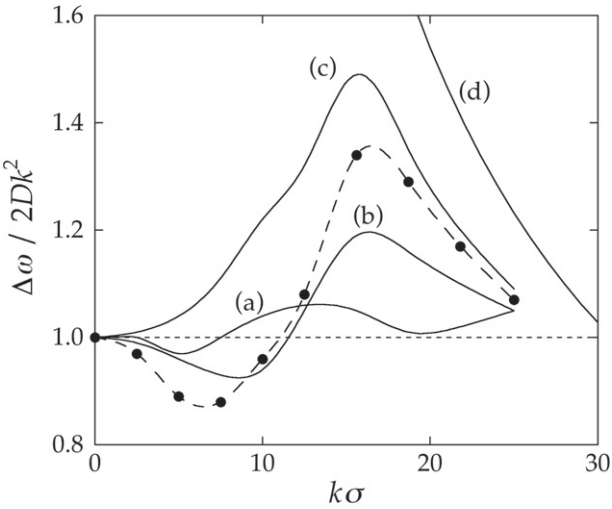

FIGURE 9.3 Width at half-height of the self dynamic structure factor relative to its value in the hydrodynamic limit. The points are molecular dynamics data for the Lennard-Jones fluid at a high density and low temperature ($\rho^* = 0.844, T^* = 0.722$) and the broken curve is drawn as an aid to the eye. The full curves show the results predicted (a) by the single-exponential approximation (9.2.18), (b) by the k-dependent generalisation of (9.2.22), (c) by the Gaussian approximation (8.2.14) and (d) in the ideal-gas ($k \to \infty$) limit. After Levesque and Verlet.[6]

single-exponential approximation (9.2.18); the same is true of the Gaussian approximation (8.2.14).

9.3 TRANSVERSE COLLECTIVE MODES

As we saw in Section 8.6, the appearance of propagating shear waves in dense fluids can be explained in qualitative or even semi-quantitative terms by a simple, viscoelastic model based on a generalisation of the hydrodynamic approach. In this section we show how such a theory can be developed in systematic fashion by use of the projection operator formalism.

Taking the viscoelastic relation (8.6.4) as a guide, we choose as components of the vector $\mathbf{A}$ the x-component of the mass current and the xz-component of the stress tensor (8.4.14), assuming as usual that the z-axis is parallel to $\mathbf{k}$. Thus

$$\mathbf{A} = \begin{pmatrix} m j_{\mathbf{k}}^{x} \\ \Pi_{\mathbf{k}}^{xz} \end{pmatrix} \tag{9.3.1}$$

and

$$(\mathbf{A}, \mathbf{A}) = V k_{\mathrm{B}} T \begin{pmatrix} \rho m & 0 \\ 0 & G_{\infty}(k) \end{pmatrix} \tag{9.3.2}$$

where $G_\infty(k)$ is the generalised elastic constant defined by (8.6.9). To calculate the frequency matrix we use the relations

$$(A_1, \dot{A}_1) = (A_2, \dot{A}_2) = 0 \tag{9.3.3}$$

$$(A_2, \dot{A}_1) = (A_1, \dot{A}_2) = -ikVk_\mathrm{B}TG_\infty(k) \tag{9.3.4}$$

and find that

$$i\boldsymbol{\Omega} = \begin{pmatrix} 0 & -ik \\ \frac{-ikG_\infty(k)}{\rho m} & 0 \end{pmatrix} \tag{9.3.5}$$

Because $\dot{A}_1$ is proportional to A_2 the projection of $\dot{A}_1$ orthogonal to $\mathbf{A}$ is identically zero. The memory function matrix therefore has only one non-zero element, which we denote by $M_t(k,t)$:

$$\mathbf{M}(k,t) = \begin{pmatrix} 0 & 0 \\ 0 & M_t(k,t) \end{pmatrix} \tag{9.3.6}$$

When these results are substituted in (9.1.40) we obtain an expression for the Laplace transform of the correlation function matrix in the form

$$\tilde{\mathbf{Y}}(k,z) = \begin{pmatrix} -iz & ik \\ \frac{ikG_\infty(k)}{\rho m} & -iz + \tilde{M}_t(k,z) \end{pmatrix}^{-1} \tag{9.3.7}$$

Thus the Laplace transform of the transverse current autocorrelation function is

$$\begin{aligned} \tilde{C}_t(k,z) &= \omega_0^2 \tilde{Y}_{11}(k,z) \\ &= \cfrac{\omega_0^2}{-iz + \cfrac{\omega_{1t}^2}{-iz + \tilde{M}_t(k,z)}} \end{aligned} \tag{9.3.8}$$

where ω_{1t}^2, defined by (7.4.38), is related to $G_\infty(k)$ by (8.6.9). Consistency with the hydrodynamic result (8.4.4) in the long-wavelength, low-frequency limit is achieved by setting

$$\tilde{M}_t(0,0) = \frac{G_\infty(0)}{\eta} \tag{9.3.9}$$

The function $\tilde{M}_t(k,z)$ is the memory function of the generalised kinematic shear viscosity introduced in Section 8.6. This identification follows immediately from comparison of of (9.3.8) with the Laplace transform of (8.6.7), which shows that

$$\tilde{C}_t(k,z) = \frac{\omega_0^2}{-iz + k^2\tilde{\nu}(k,z)} \tag{9.3.10}$$

The viscoelastic approximation corresponds to ignoring the frequency dependence of $\tilde{M}_t(k,z)$ and replacing it by a constant, $1/\tau_t(k)$ say, implying that

$\nu(k,t)$ decays exponentially with a characteristic time $\tau_t(k)$ and hence, from (8.6.9), that

$$\nu(k,t) = \frac{G_\infty(k)}{\rho m} \exp[-|t|/\tau_t(k)] \tag{9.3.11}$$

Use of (9.3.11) ensures that the spectrum of transverse current fluctuations:

$$C_t(k,\omega) = \frac{1}{\pi} \operatorname{Re} \tilde{C}_t(k,\omega) = \frac{1}{\pi} \frac{\omega_0^2 \omega_{1t}^2 \tau_t(k)}{\omega^2 + \tau_t^2(k)(\omega_{1t}^2 - \omega^2)^2} \tag{9.3.12}$$

has the correct second moment irrespective of the choice of $\tau_t(k)$. If, as in Section 8.6, we define a wavenumber-dependent shear viscosity $\eta(k)$ as the zero-frequency limit of $\rho m \tilde{\nu}(k,\omega)$, we find in the approximation represented by (9.3.11) that

$$\eta(k) = \tau_t(k) G_\infty(k) \tag{9.3.13}$$

so that $\tau_t(k)$ appears as a wavenumber-dependent Maxwell relaxation time (see (8.6.5)). In particular:

$$\eta \equiv \eta(0) = \tau_t(0) G_\infty(0) \tag{9.3.14}$$

in agreement with (9.3.9).

It is easy to establish the criterion for the existence of propagating transverse modes within the context of the approximation represented by (9.3.12), characterised by a single relaxation time. The condition for $C_t(k,\omega)$ to have a peak at non-zero frequency at a given value of k is

$$\omega_{1t}^2 \tau_t^2(k) > \frac{1}{2} \tag{9.3.15}$$

and the peak, if it exists, is at a frequency ω such that $\omega^2 = \omega_{1t}^2 - \frac{1}{2}\tau_t^{-2}(k)$. It follows from the inequality (9.3.15) that shear waves will appear for values of k greater than k_c, where k_c is a critical wavevector given by

$$k_c^2 = \frac{\rho m}{2\tau_t^2(k) G_\infty(k)} \tag{9.3.16}$$

We can obtain an estimate for k_c by taking the $k \to 0$ limit of (9.3.16); this gives

$$k_c^2 \approx \frac{\rho m G_\infty(0)}{2\eta^2} \tag{9.3.17}$$

On inserting the values of η and $G_\infty(0)$ obtained by molecular dynamics calculations for the Lennard-Jones fluid close to its triple point we find that $k_c\sigma \approx 0.79$. This is apparently a rather good guide to what occurs in practice: the dispersion curve for liquid argon plotted in Figure 8.4 shows that shear waves first appear at $k_c \approx 2.0$ Å or, taking a value (3.4 Å) for σ appropriate to argon, $k_c\sigma \approx 0.7$. At sufficiently large values of k the shear-waves disappear again as the role of the interparticle forces becomes less important.

Given its simplicity, the viscoelastic approximation provides a satisfactory description of the transverse current fluctuations over a wide range of

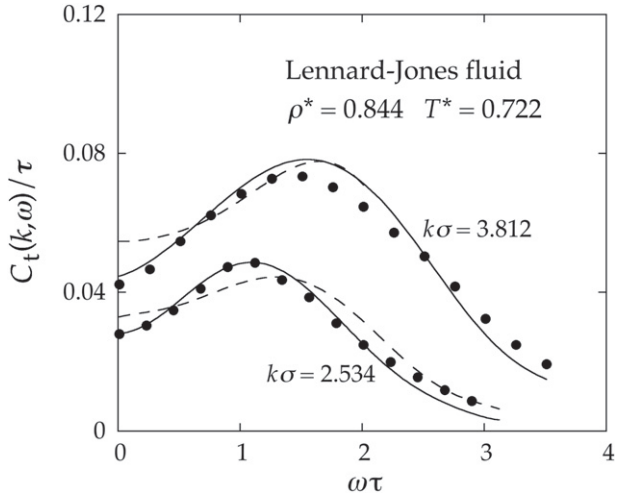

FIGURE 9.4 Spectrum of transverse-current fluctuations for the Lennard-Jones fluid near its triple point. The points are molecular dynamics results and the curves show results calculated from the viscoelastic approximation (9.3.11) (broken lines) and the two-exponential memory function (9.3.20) (full lines). The unit of time is $\tau = (m\sigma^2/48\epsilon)^{1/2}$. *Redrawn with permission from Ref. 7* © *1973 American Physical Society.*

wavelength. Careful study reveals, however, that there are some systematic discrepancies with the molecular dynamics data that persist even when the parameter $\tau_t(k)$ is chosen to fit the observed spectrum rather than calculated from some semi-empirical prescription. In particular, the shear-wave peaks at long wavelengths are significantly too broad and flat, as the results for the Lennard-Jones fluid shown in Figure 9.4 reveal. The structure of the correlation function matrix (9.3.7) provides a clue as to the origin of the deficiencies in the viscoelastic model. The element $\tilde{Y}_{22}(k,z)$ of the matrix is the Laplace transform of the normalised autocorrelation function of the xz-component of the stress tensor. Thus

$$\begin{aligned}\tilde{Y}_{22}(k,z) &= \frac{\beta}{VG_\infty(k)}\int_0^\infty \left\langle \Pi^{xz}_{\mathbf{k}}(t)\Pi^{xz}_{-\mathbf{k}}\right\rangle \exp(izt)\mathrm{d}t \\ &= \frac{1}{-iz + \tilde{M}_t(k,z) + \dfrac{\omega_{1t}^2}{-iz}}\end{aligned} \tag{9.3.18}$$

where the form of the normalisation factor follows from (8.4.10) and (8.6.9). If we again replace $\tilde{M}_t(k,z)$ by $1/\tau_t(k)$ and take the limit $k \to 0$, (9.3.18) can be inverted to give

$$\eta(t) = G_\infty(0)Y_{22}(0,t) = G_\infty(0)\exp[-G_\infty(0)|t|/\eta] \tag{9.3.19}$$

which is consistent with (8.4.10). We saw in Section 8.6 that the memory function $\nu(k,t)$ and the stress autocorrelation function $\eta(t)$ become identical (apart

from a multiplicative factor) as k tends to zero; within the viscoelastic approximation the identity is apparent immediately from intercomparison of (9.3.11), (9.3.14) and (9.3.19). At high densities, as Figure 8.3 illustrates, the correlation function $\eta(t)$ has a pronounced, slowly decaying tail and it is reasonable to suppose that the transverse current fluctuations at small wavevectors can be adequately described only if a comparably long-lived contribution is included in the memory function $\nu(k,t)$. In their classic analysis of the collective dynamical properties of the Lennard-Jones fluid, Levesque et al.[7] suggested the use of of a two-exponential memory function of the form

$$\nu(k,t)/\nu(k,0) = (1-\alpha_k)\exp[-|t|/\tau_1(k)] + \alpha_k \exp[-|t|/\tau_2(k)] \quad (9.3.20)$$

which, as the discussion of the results in Figure 8.3 suggests, is also a useful approximation for other potential models. In practice, for the Lennard-Jones fluid, the slow relaxation time τ_2 turns out to be almost independent of k and some seven times larger than $\tau_1(0)$, while the parameter α_k, which at the smallest wavenumber studied has a value of approximately 0.1, decreases rapidly with increasing k. Thus, for large k, the single relaxation time approximation is recovered. At small k, however, inclusion of the long-lived tail in the memory function leads to a marked enhancement of the shear-wave peaks and significantly improved agreement with the molecular dynamics results, as illustrated in Figure 9.4; the price paid is the introduction of an additional two parameters. Broadly similar conclusions have emerged from calculations for liquid metals.[8]

9.4 DENSITY FLUCTUATIONS

The description of the longitudinal current fluctuations on the basis of the generalised Langevin equation is necessarily a more complicated task than in the case of the transverse modes. This is obvious from the much more complicated structure of the hydrodynamic formula (8.5.10) compared with (8.4.4). The problem of particular interest is to account for the dispersion and eventual disappearance of the collective mode associated with sound-wave propagation.

In discussion of the longitudinal modes a natural choice of components of the dynamical vector $\mathbf{A}$ is the set of conserved variables consisting of $\rho_{\mathbf{k}}$, $\mathbf{j}_{\mathbf{k}}$ and the microscopic energy density $e_{\mathbf{k}}$ defined via (8.5.27). The variables $\rho_{\mathbf{k}}$ and $e_{\mathbf{k}}$ are both orthogonal to $\mathbf{j}_{\mathbf{k}}$. In place of $e_{\mathbf{k}}$, however, it is more convenient to choose that part which is also orthogonal to $\rho_{\mathbf{k}}$ and plays the role of a microscopic temperature fluctuation; this we write as $T_{\mathbf{k}}$. Thus

$$T_{\mathbf{k}} = e_{\mathbf{k}} - (\rho_{\mathbf{k}}, e_{\mathbf{k}})(\rho_{\mathbf{k}}, \rho_{\mathbf{k}})^{-1}\rho_{\mathbf{k}} \quad (9.4.1)$$

The static correlation matrix is then diagonal. Since our attention is focused on the longitudinal fluctuations, we include only the projection of the current

along $\mathbf{k}$, which we label $j^z_{\mathbf{k}}$. The vector $\mathbf{A}$ specified in this way, i.e.

$$\mathbf{A} = \begin{pmatrix} \rho_{\mathbf{k}} \\ j^z_{\mathbf{k}} \\ T_{\mathbf{k}} \end{pmatrix} \tag{9.4.2}$$

is only one of many possible choices; larger sets of variables that include both the stress tensor and heat current have also been considered. The static correlation matrix arising from (9.4.2) is

$$(\mathbf{A}, \mathbf{A}) = \begin{pmatrix} NS(k) & 0 & 0 \\ 0 & \dfrac{Nk_{\mathrm{B}}T}{m} & 0 \\ 0 & 0 & \langle T_{\mathbf{k}} T_{-\mathbf{k}} \rangle \end{pmatrix} \tag{9.4.3}$$

and the corresponding frequency matrix is

$$-i\boldsymbol{\Omega} = \begin{pmatrix} 0 & -ik & 0 \\ \dfrac{-ik}{S(k)}\left(\dfrac{k_{\mathrm{B}}T}{m}\right) & 0 & \dfrac{\langle \dot{j}^z_{\mathbf{k}} T_{-\mathbf{k}} \rangle}{\langle T_{\mathbf{k}} T_{-\mathbf{k}} \rangle} \\ 0 & -\dfrac{\langle T_{\mathbf{k}} \dot{j}^z_{-\mathbf{k}} \rangle}{Nk_{\mathrm{B}}T/m} & 0 \end{pmatrix} \tag{9.4.4}$$

It is unnecessary for our purposes to write more explicit expressions for the statistical averages appearing in (9.4.3) and (9.4.4).

Since $\dot{A}_1$ is proportional to A_2, it follows that the component R_1 of the random-force vector is zero and the memory function matrix reduces to

$$\mathbf{M}(k,t) = \begin{pmatrix} 0 & 0 & 0 \\ 0 & M_{22}(k,t) & M_{23}(k,t) \\ 0 & M_{32}(k,t) & M_{33}(k,t) \end{pmatrix} \tag{9.4.5}$$

The correlation function matrix is therefore given by

$$\tilde{\mathbf{Y}}(k,z) = \begin{pmatrix} -iz & ik & 0 \\ \dfrac{ik}{S(k)}\left(\dfrac{k_{\mathrm{B}}T}{m}\right) & -iz + \tilde{M}_{22}(k,z) & -i\Omega_{23} + \tilde{M}_{23}(k,z) \\ 0 & -i\Omega_{32} + \tilde{M}_{32}(k,z) & -iz + \tilde{M}_{33}(k,z) \end{pmatrix}^{-1} \tag{9.4.6}$$

and the Laplace transform of the longitudinal current autocorrelation function is

$$\tilde{C}_l(k,z) = \omega_0^2 \tilde{Y}_{22}(k,z) = \frac{\omega_0^2}{-iz + \dfrac{\omega_0^2}{-izS(k)} + \tilde{N}_l(k,z)} \tag{9.4.7}$$

where the memory function $N_l(k,t)$ is defined through its Laplace transform as

$$\tilde{N}_l(k,z) = \tilde{M}_{22}(k,z) - \frac{\Theta(k,z)}{-iz + \tilde{M}_{33}(k,z)} \tag{9.4.8}$$

with

$$\Theta(k,z) = \left(\tilde{M}_{23}(k,z) - \frac{\langle \dot{j}^z_{\mathbf{k}} T_{-\mathbf{k}}\rangle}{\langle T_{\mathbf{k}} T_{-\mathbf{k}}\rangle}\right)\left(\tilde{M}_{32}(k,z) + \frac{\langle T_{\mathbf{k}} \dot{j}^z_{-\mathbf{k}}\rangle}{N(k_B T/m)}\right) \tag{9.4.9}$$

The physical significance of the four unknown memory functions in (9.4.5) can be inferred from their definitions in terms of the random forces $\mathcal{Q}\dot{j}^z_{\mathbf{k}}$ and $\mathcal{Q}\dot{T}_{\mathbf{k}}$. The functions M_{23} and M_{32} describe a coupling between the momentum current (the stress tensor) and heat flux whereas M_{22} and M_{33} represent, respectively, the relaxation processes associated with viscosity and thermal conduction. By comparison of (9.4.7)–(9.4.9) with the hydrodynamic result in (8.5.10) we can make the following identifications in the limit $k \to 0$:

$$\lim_{k\to 0} \tilde{M}_{22}(k,0) = \frac{\left(\frac{4}{3}\eta + \zeta\right)k^2}{\rho m} = bk^2 \tag{9.4.10}$$

$$\lim_{k\to 0} \tilde{M}_{33}(k,0) = \frac{\lambda k^2}{\rho c_V} = ak^2 \tag{9.4.11}$$

and

$$\lim_{k\to 0} \frac{|\langle \dot{j}^z_{\mathbf{k}} T_{-\mathbf{k}}\rangle|^2}{\langle T_{\mathbf{k}} T_{-\mathbf{k}}\rangle} = Nk^2\left(\frac{k_B T}{m}\right)^2 \frac{\gamma - 1}{S(k)} \tag{9.4.12}$$

Finally, by requiring that

$$N_l(k, t=0) = \omega_{1l}^2 - \frac{\omega_0^2}{S(k)} \tag{9.4.13}$$

with ω_{1l}^2 given by (7.4.35), we guarantee that the first three non-zero moments of $S(k,\omega)$ are correct.

The derivation of (9.4.6) brings out clearly the advantage of working with a multi-variable description of a problem, such as that provided by (9.4.2). For example, we can immediately write down an expression for the fluctuations in temperature analogous to (9.4.7) for the current fluctuations. If we define a temperature autocorrelation function as

$$C_T(k,t) = \langle T_{\mathbf{k}}(t) T_{-\mathbf{k}}\rangle \tag{9.4.14}$$

we find from (9.4.6) that

$$\begin{aligned}\tilde{C}_T(k,z) &= \langle T_{\mathbf{k}} T_{-\mathbf{k}}\rangle\, \tilde{Y}_{33}(k,z) \\ &= \frac{\langle T_{\mathbf{k}} T_{-\mathbf{k}}\rangle}{-iz - \dfrac{\Theta(k,z)}{-iz + \dfrac{\omega_0^2}{-izS(k)} + \tilde{M}_{22}(k,z)} + \tilde{M}_{33}(k,z)}\end{aligned} \tag{9.4.15}$$

The key point to note is that $\tilde{C}_T(k,z)$ can be expressed in terms of the same memory functions used to describe $\tilde{C}_l(k,z)$. Similarly, by solving for $\tilde{Y}_{11}(k,z)$, we obtain an expression for the density autocorrelation function:

$$\tilde{F}(k,z) = S(k)\tilde{Y}_{11}(k,z) = \frac{S(k)}{-iz + \dfrac{1}{S(k)}\left(\dfrac{\omega_0^2}{-iz + \tilde{N}_l(k,z)}\right)} \tag{9.4.16}$$

This is a less interesting result than that obtained for $\tilde{C}_T(k,z)$ because $F(k,t)$ and $C_l(k,t)$ are in any case related by (7.4.26). It nevertheless brings out a second important feature of the multi-variable approach. An expression for $\tilde{F}(k,z)$ having the same form as (9.4.16) can more easily be obtained by setting $A = \rho_{\mathbf{k}}$ and making a continued-fraction expansion of $\tilde{F}(k,z)$ truncated at second order. What the more elaborate calculation yields is detailed information on the structure of the memory function $N_l(k,t)$, enabling contact to be made with the hydrodynamic result and allowing approximations to be introduced in a controlled way.

If we write the complex function $\tilde{N}_l(k,z)$ on the real axis ($z = \omega + i\epsilon, \epsilon \to 0+$) as the sum of its real and imaginary parts, i.e.

$$\tilde{N}_l(k,\omega) = N_l'(k,\omega) + iN_l''(k,\omega) \tag{9.4.17}$$

we find from (9.4.7) that the spectrum of longitudinal current fluctuations is given by

$$C_l(k,\omega) = \frac{1}{\pi}\frac{\omega^2\omega_0^2 N_l'(k,\omega)}{[\omega^2 - \omega_0^2/S(k) - \omega N_l''(k,\omega)]^2 + [\omega N_l'(k,\omega)]^2} \tag{9.4.18}$$

If the memory function were small, there would be a resonance at a frequency determined by the static structure of the fluid, i.e. at $\omega^2 \approx \omega_0^2/S(k)$. The physical role of the memory function – the generalised 'friction' – is therefore to shift and damp the resonance.

The task of calculating the function $N_l(k,t)$ remains a formidable one, even with the restrictions we have discussed. Some recourse to modelling is therefore needed if tractable expressions for $C_l(k,\omega)$ and $S(k,\omega)$ are to be obtained. The limiting form of $\tilde{N}_l(k,\omega)$ when $k,\omega \to 0$ (the hydrodynamic limit) follows from (9.4.8)–(9.4.12):

$$\lim_{\omega\to 0}\lim_{k\to 0}\tilde{N}_l(k,\omega) = bk^2 + \frac{\omega_0^2}{S(k)}\frac{\gamma - 1}{-i\omega + ak^2} \tag{9.4.19}$$

The first term on the right-hand side of this expression describes viscous relaxation and corresponds to $\tilde{M}_{22}(k,\omega)$ in (9.4.8), while the second term arises from temperature fluctuations. We now require a generalisation of (9.4.19) that is valid for microscopic wavelengths and frequencies. An obvious first approximation is to assume that the coupling between the momentum and heat currents, represented by the memory functions $M_{23}(k,t)$ and $M_{32}(k,t)$, makes

no contribution to the density fluctuations. This is true in the hydrodynamic limit and it is true instantaneously at finite wavelengths because the random forces $\mathcal{Q}\dot{j}^z_{\mathbf{k}}$ and $\mathcal{Q}\dot{T}_{\mathbf{k}}$ are instantaneously uncorrelated; the two memory functions therefore vanish at $t = 0$. If we also assume that the effect of thermal fluctuations is negligible, an approximation that can be justified at large wavenumbers, we are left only with the problem of representing the generalised longitudinal viscosity $\tilde{M}_{22}(k, \omega)$. Since the viscoelastic model (9.3.11) works moderately well in the case of the transverse currents, it is natural to make a similar approximation here by writing

$$N_l(k, t) = \left(\omega_{1l}^2 - \frac{\omega_0^2}{S(k)}\right) \exp[-|t|/\tau_l(k)] \tag{9.4.20}$$

which is compatible with the constraint (9.4.13). The resulting expression for the dynamic structure factor is

$$S(k, \omega) = \frac{1}{\pi} \frac{\tau_l(k)\omega_0^2[\omega_{1l}^2 - \omega_0^2/S(k)]}{\omega^2\tau_l^2(k)(\omega^2 - \omega_{1l}^2)^2 + [\omega^2 - \omega_0^2/S(k)]^2} \tag{9.4.21}$$

A variety of proposals have been made for the calculation of the relaxation time $\tau_l(k)$. For example, arguments similar to those used in the derivation of (9.2.21) lead in this case to the expression[9]

$$\tau_l^{-1}(k) = \frac{2}{\pi^{1/2}} \left(\omega_{1l}^2 - \frac{\omega_0^2}{S(k)}\right)^{1/2} \tag{9.4.22}$$

The usefulness of this approach is illustrated[11] in Figure 9.5, which shows the dispersion of the sound wave peak obtained from molecular dynamics calculations for liquid rubidium and compares the results with those predicted by the viscoelastic approximation (9.4.21) in conjunction with (9.4.22). The agreement is good but the detailed shape of $S(k, \omega)$ is less well reproduced, particularly at small k. As the example shown in Figure 9.6 reveals, the discrepancies occur mostly at low frequencies. This is not surprising, since the low-frequency region of the spectrum is dominated by temperature fluctuations, which the viscoelastic model ignores.

The type of scheme outlined above is clearly an oversimplification and one that fails badly in the case of the Lennard-Jones fluid, where it cannot explain the appearance of the Brillouin peak seen in molecular dynamics calculations, an example of which is pictured in Figure 9.7. It can be shown from (9.4.22) that the viscoelastic model predicts the existence of a propagating mode at values of k such that

$$\omega_{1l}^2 < \frac{3\omega_0^2}{S(k)} \tag{9.4.23}$$

If k is small this inequality can be rewritten as

$$\chi_T \left[\frac{4}{3}G_\infty(0) + K_\infty(0)\right] < 3 \tag{9.4.24}$$

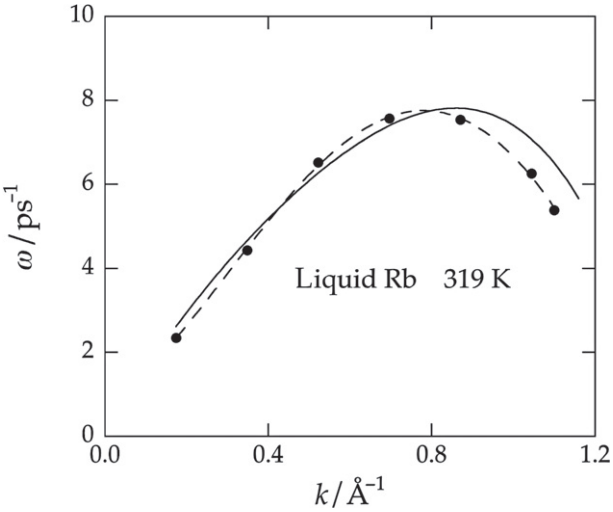

FIGURE 9.5 Sound-wave dispersion curve for a model of liquid rubidium near the normal melting temperature. The points are molecular dynamics results[10] and the broken curve is drawn as a guide to the eye. The full curve is calculated from the viscoelastic approximation (9.4.21) in conjunction with (9.4.22). From J.R.D. Copley and S.W. Lovesey, 'The dynamic properties of monatomic liquids', *Rep. Prog. Phys.* **38**, 461–563 (1975). *© IOP Publishing 1975. Reproduced by permission of IOP Publishing. All rights reserved.*

when ω_{1l}^2 is expressed in terms of the long-wavelength limits of the instantaneous shear modulus (8.6.9) and the instantaneous bulk modulus $K_\infty(k)$ defined by the relation

$$\frac{4}{3}G_\infty(k) + K_\infty(k) = \frac{\rho m \omega_{1l}^2}{k^2} \tag{9.4.25}$$

In the case of the alkali metals the inequality (9.4.24) is easily satisfied, but for the Lennard-Jones fluid under triple-point conditions the left-hand side of (9.4.24) has a value of ≈4.9. Given the structure of (9.4.24), it seems plausible to conclude that the fact that the sound-wave peak in liquid metals is found to persist to larger wavenumbers than in rare-gas liquids is associated with the lower compressibility of the metals (see Table 1.2). This difference in behaviour can in turn be correlated with the softer nature of the interatomic potentials in metals compared with those in the rare gases.

In order to describe the small-k behaviour of the Lennard-Jones system it is necessary to go beyond the viscoelastic approximation (9.4.20) by including the effect of temperature fluctuations. A generalisation of the hydrodynamic result (9.4.19) that satisfies the short-time constraint (9.4.13) is obtained by setting

$$\tilde{N}_l(k,\omega) = \left(\omega_{1l}^2 - \frac{\omega_0^2 \gamma(k)}{S(k)}\right)\tilde{n}_{1l}(k,\omega) + \frac{\omega_0^2}{S(k)}\frac{\gamma(k)-1}{-i\omega + a(k)k^2} \tag{9.4.26}$$

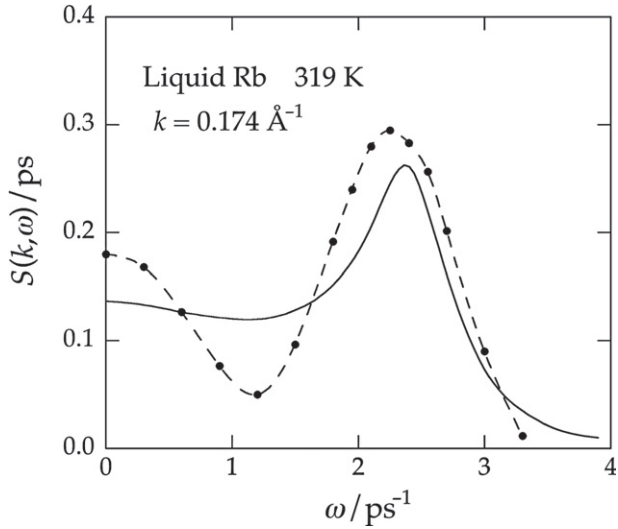

FIGURE 9.6 Dynamic structure factor at a wavenumber $k = 0.174$ Å^{-1} for a model of liquid rubidium near the normal melting temperature. The points are molecular dynamics results[10] and the broken curve is drawn as a guide to the eye. The full curve is calculated from the viscoelastic approximation (9.4.21) in conjunction with (9.4.22). From J.R.D. Copley and S.W. Lovesey, 'The dynamic properties of monatomic liquids', *Rep. Prog. Phys.* **38**, 461–563 (1975). *© IOP Publishing 1975. Reproduced by permission of IOP Publishing. All rights reserved.*

with $n_{1l}(k, t = 0) = 1$; this ignores any frequency dependence of the generalised thermal diffusivity $a(k)$ (the quantity $a(0)$ is defined by (8.3.14)). If, in addition, $\gamma(k)$ (a k-dependent ratio of specific heats) is set equal to one, the term representing temperature fluctuations disappears and (9.4.26) reduces to the viscoelastic approximation; the latter, as we have seen, works reasonably well for liquid metals, for which $\gamma(0) \approx 1$ (see Table 1.2). The first term on the right-hand side of (9.4.26) can be identified as $\tilde{M}_{22}(k, \omega)$. Then, if we assume a simple, exponential form for $n_{1l}(k, t)$, i.e.

$$n_{1l}(k, t) = \exp\big[- |t|/\tau_l(k)\big] \tag{9.4.27}$$

we find that in the hydrodynamic limit $\tilde{M}_{22}(k, 0)$ approaches the value

$$\lim_{k\to 0} \frac{\tilde{M}_{22}(k,0)}{k^2} = \frac{\tau_l(0)}{\rho m}\left[\frac{4}{3}G_\infty(0) + K_\infty(0) - \gamma/\chi_T\right] \tag{9.4.28}$$

Comparison of (9.4.28) with (9.4.10) shows that $\tau_l(0)$ is given by

$$\tau_l(0) = \frac{\frac{4}{3}\eta + \zeta}{\frac{4}{3}G_\infty(0) + K_\infty(0) - \gamma/\chi_T} \tag{9.4.29}$$

Equations (9.4.26)–(9.4.29) make up the set of generalised hydrodynamic equations used by Levesque et al.[7] in their study of the Lennard-Jones fluid; together they yield a good fit to the dynamic structure factor over a wide range of k. Among the satisfying features of the analysis is the fact that at long wavelengths $\tau_l(k)$, as determined by a least-squares fitting procedure, tends correctly to its limiting value (9.4.29) as $k \to 0$. Moreover, $\gamma(k) \approx 1$ beyond $k\sigma \approx 2$. The large-k behaviour of $\gamma(k)$ implies that the viscoelastic model is a good approximation at short wavelengths because the coupling with the thermal mode becomes negligible. On the other hand, at small k, $\gamma(k)$ tends to a value that is greater by a factor of ≈ 2 than the thermodynamic value derived from the simulation, $\gamma = 1.86 \pm 0.01$. This fault can be eliminated by inclusion of a slowly relaxing part in the generalised longitudinal viscosity $\tilde{M}_{22}(k,\omega)$. If a two-exponential form is used for $n_{1l}(k,t)$, with the two decay times $\tau_1(k)$ (fast) and $\tau_2(k)$ (slow) given the same values[12] and the two terms in the memory function given the same relative weight as in the transverse current memory function (9.3.20), a very good fit is obtained, as Figure 9.7 shows, for which $\gamma(k)$ tends to its thermodynamic value as $k \to 0$. The agreement obtained with a single exponential is to some extent fortuitous. At small k the relaxation time $1/a(k)k^2$ associated with the thermal term in (9.4.26) is similar in value to the slow relaxation time τ_2. The omission of the long-time part of the viscous

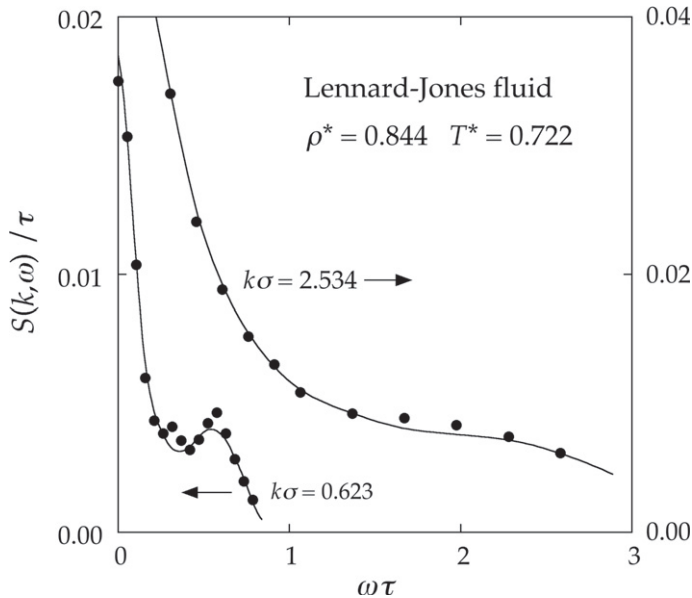

FIGURE 9.7 Dynamic structure factor of the Lennard-Jones fluid near its triple point. The points are molecular dynamics results and the curves show results calculated from (9.4.26) with a two-exponential approximation to $n_{1l}(k,t)$. The unit of time is $\tau = (m\sigma^2/48\epsilon)^{1/2}$. *Redrawn with permission from Ref. 7 © 1973 American Physical Society.*

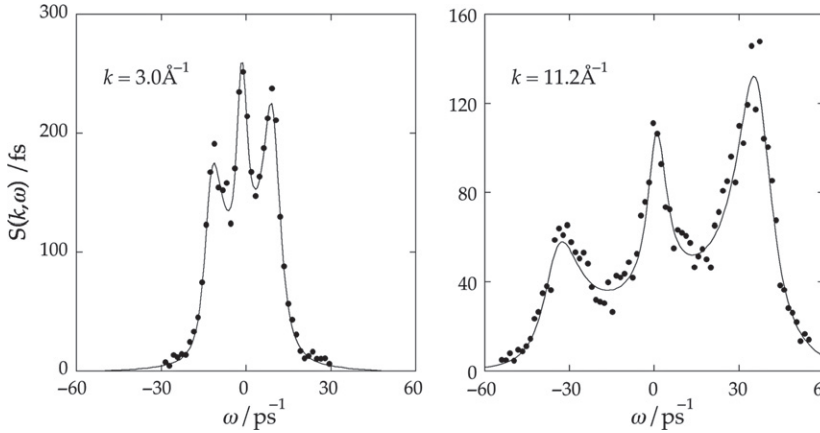

FIGURE 9.8 Dynamic structure factor of liquid lithium at 475 K for two values of k. The points are the results of inelastic X-ray scattering experiments and the curves show results calculated from (9.4.26) with a two-exponential approximation to $n_{1l}(k,t)$ and the experimental values of γ and a. *Redrawn with permission from Ref. 13 © 2000 American Physical Society.*

contribution to the memory function can therefore be offset, at least in part, by an increase in the size of the thermal contribution.

The slowly decaying contribution to the memory function is most important at those values of k for which a propagating mode is seen; at shorter wavelengths the dynamic structure factor is well described by a simpler, rapidly decaying, memory function. Calculations for the alkali metals therefore provide a more severe test of the need to include the contributions from both fast and slow processes, since the wavenumber range over which the Brillouin peaks are detectable is considerably wider than it is for argon-like liquids. The high quality data provided by inelastic X-ray scattering experiments make such a test possible. Figure 9.8 shows some results of X-ray measurements[13] on liquid lithium, together with those derived from a memory function having the same form as that used in the work on the Lennard-Jones fluid, again with an approximation for $n_l(k,t)$ involving two significantly different time scales; to allow direct comparison with the experimental data the theoretical results have been modified to allow for detailed balance (see (7.5.15)) and instrumental resolution. One important difference compared with the earlier work is the fact that the very high thermal conductivity of a liquid metal means that at wavenumbers relevant to X-ray scattering experiments the thermal contribution to the memory function is essentially a delta-function in time. A different fitting procedure was also used, in which the relaxation times and the relative weight attached to the fast and slow contributions, all taken to be functions of k, were treated as free parameters. The agreement between theory and experiment is very good and significantly better than that obtained with a single relaxation time. Inclusion of the long-lived term is necessary in order to reproduce the high

degree of structure seen in the experimental results. At small wavenumbers the two relaxation times were found to differ by roughly an order of magnitude, with the weight of the slow process being 5–10 times smaller than that of the faster one, results which are broadly consistent with those obtained for the Lennard-Jones fluid. Similar conclusions have emerged from the analysis of X-ray scattering experiments for a number of other liquid metals.[14]

9.5 MODE COUPLING THEORY I. THE VELOCITY AUTOCORRELATION FUNCTION

The applications of the projection operator formalism studied thus far are largely phenomenological in character in the sense that a simple functional form has generally been assumed to describe the decay of the various memory functions. Such descriptions may be looked upon as interpolation schemes between the short-time behaviour of correlation functions, which is introduced via frequency sum rules, and the hydrodynamic regime, which governs the choice of dynamical variables to be included in the vector **A**. A more ambitious programme would be to derive expressions for the memory functions from first principles, starting from the formally exact definitions of Section 9.1. A possible route towards such a microscopic theory is provided by the mode coupling approach, which we have already used in Section 8.7 to investigate the slow decay of the velocity autocorrelation function at long times. In this section we show how mode coupling concepts can be applied to the calculation of time correlation functions and their associated memory functions within the framework of the projection operator approach. The basic idea behind mode coupling theory is that a fluctuation (or 'excitation') in a given dynamical variable decays predominantly into pairs of hydrodynamic modes associated with conserved single-particle or collective dynamical variables. The possible 'decay channels' of a fluctuation are determined by 'selection rules' based, for example, on time reversal symmetry or on physical considerations. If a further, decoupling approximation is made, time correlation functions become expressible as sums of products of the correlation functions of conserved variables.

To illustrate the method we shall first rederive the asymptotic form (8.7.15) of the velocity autocorrelation function. Let u_{ix} be the x-component of the velocity of a tagged particle i. In the notation of Section 9.1 the velocity autocorrelation function has the from

$$Z(t) = \left(u_{ix}, \exp\left(i\mathcal{L}t\right)u_{ix}\right) \tag{9.5.1}$$

From the discussion in Section 8.7 we can expect the tagged-particle velocity to be strongly coupled to the longitudinal and transverse components of the collective particle current, while the form of (8.7.8) suggests that we take the tagged-particle density $\rho_{\mathbf{k}'i}$ and the current $\mathbf{j}_{-\mathbf{k}''}$ to be the modes into which fluctuations in u_{ix} decay. Translational invariance implies that the only products

of Fourier components whose inner product with the tagged-particle velocity are non-zero are those for which $\mathbf{k}' = \mathbf{k}''$. The first approximation of the mode coupling treatment therefore consists in replacing the full evolution operator $\exp(i\mathcal{L}t)$ by its projection onto the subspace of the product variables $\rho_{\mathbf{k}i}\mathbf{j}_{-\mathbf{k}}$, i.e.

$$\exp(i\mathcal{L}t) \approx \mathcal{P}\exp(i\mathcal{L}t)\mathcal{P} \tag{9.5.2}$$

The projection operator $\mathcal{P}$ is defined, as in (9.1.1), by its action on a dynamical variable B:

$$\mathcal{P}B = \sum_{\mathbf{k}}\sum_{\alpha}\left(\rho_{\mathbf{k}i}\, j^{\alpha}_{-\mathbf{k}}, B\right)\left(\rho_{\mathbf{k}i}\, j^{\alpha}_{-\mathbf{k}}, \rho_{\mathbf{k}i}\, j^{\alpha}_{-\mathbf{k}}\right)^{-1}\rho_{\mathbf{k}i}\, j^{\alpha}_{-\mathbf{k}} \tag{9.5.3}$$

where the sum on α runs over all Cartesian components. Thus

$$\begin{aligned}\exp(i\mathcal{L}t)\mathcal{P}u_{ix} = &\sum_{\mathbf{k}'}\sum_{\beta}\left(\rho_{\mathbf{k}'i}\, j^{\beta}_{-\mathbf{k}'}, u_{ix}\right)\left(\rho_{\mathbf{k}'i}\, j^{\beta}_{-\mathbf{k}'}, \rho_{\mathbf{k}'i}\, j^{\beta}_{-\mathbf{k}'}\right)^{-1}\\ &\times\exp(i\mathcal{L}t)\rho_{\mathbf{k}'i}\, j^{\beta}_{-\mathbf{k}'}\end{aligned} \tag{9.5.4}$$

and

$$\begin{aligned}Z(t) &\approx \left(u_{ix}, \mathcal{P}\exp(i\mathcal{L}t)\mathcal{P}u_{ix}\right)\\ &= \sum_{\mathbf{k},\mathbf{k}'}\sum_{\alpha}\sum_{\beta}\left(\rho_{\mathbf{k}'i}\, j^{\beta}_{-\mathbf{k}'}, u_{ix}\right)\left(\rho_{\mathbf{k}'i}\, j^{\beta}_{-\mathbf{k}'}, \rho_{\mathbf{k}'i}\, j^{\beta}_{-\mathbf{k}'}\right)^{-1}\\ &\quad\times\left(\rho_{\mathbf{k}i}\, j^{\alpha}_{-\mathbf{k}}, \exp(i\mathcal{L}t)\rho_{\mathbf{k}'i}\, j^{\beta}_{-\mathbf{k}'}\right)\\ &\quad\times\left(\rho_{\mathbf{k}i}\, j^{\alpha}_{-\mathbf{k}}, \rho_{\mathbf{k}i}\, j^{\alpha}_{-\mathbf{k}}\right)^{-1}\left(u_{ix}, \rho_{\mathbf{k}i}\, j^{\alpha}_{-\mathbf{k}}\right)\end{aligned} \tag{9.5.5}$$

In this expression the time correlation functions of the product variables are bracketed by two, time-independent 'vertices', each of which has the same value. For example, since $\left\langle\rho_{\mathbf{k}i}\, j^{\alpha}_{-\mathbf{k}}\rho_{-\mathbf{k}i}\, j^{\alpha}_{\mathbf{k}}\right\rangle = N(k_{\mathrm{B}}T/m)$ and $\left\langle u_{ix}\rho_{-\mathbf{k}i}\, j^{\alpha}_{\mathbf{k}}\right\rangle = (k_{\mathrm{B}}T/m)\delta_{\alpha x}$, it follows that

$$\left(\rho_{\mathbf{k}i}\, j^{\alpha}_{-\mathbf{k}}, \rho_{\mathbf{k}i}\, j^{\alpha}_{-\mathbf{k}}\right)^{-1}\left(u_{ix}, \rho_{\mathbf{k}i}\, j^{\alpha}_{-\mathbf{k}}\right) = \frac{1}{N}\delta_{\alpha x} \tag{9.5.6}$$

The time correlation functions appearing on the right-hand side of (9.5.5) are of an unusual type, since they involve four, rather than two, dynamical variables. A second approximation usually made is to assume that the two modes appearing in the product variables propagate independently of each other. This means that the four-variable functions factorise into products of two-variable functions. In the present case:

$$\begin{aligned}\left(\rho_{\mathbf{k}i}\, j^{\alpha}_{-\mathbf{k}}, \exp(i\mathcal{L}t)\rho_{\mathbf{k}'i}\, j^{\beta}_{-\mathbf{k}'}\right) &\approx \left(\rho_{\mathbf{k}i}, \exp(i\mathcal{L}t)\rho_{\mathbf{k}'i}\right)\left(j^{\alpha}_{-\mathbf{k}}, \exp(i\mathcal{L}t)\, j^{\beta}_{-\mathbf{k}'}\right)\delta_{\mathbf{k}\mathbf{k}'}\\ &\equiv \left\langle\rho_{\mathbf{k}i}(t)\rho_{-\mathbf{k}i}\right\rangle\left\langle j^{\beta}_{-\mathbf{k}}(t)\, j^{\alpha}_{\mathbf{k}}\right\rangle\end{aligned} \tag{9.5.7}$$

and use of (9.5.6) and (9.5.7) reduces (9.5.5) to the simpler form given by

$$Z(t) = \frac{1}{N^2} \sum_{\mathbf{k}} \langle \rho_{\mathbf{k}i}(t) \rho_{-\mathbf{k}i} \rangle \left\langle j^x_{\mathbf{k}}(t) j^x_{-\mathbf{k}} \right\rangle \tag{9.5.8}$$

The first factor in the sum over wavevectors is the self intermediate scattering function $F_s(k,t)$ and the second is a current correlation function; the latter can be decomposed into its longitudinal and transverse parts in the manner of (7.4.24). On switching from a sum to an integral and replacing the current correlation function by its average over a sphere, (9.5.8) becomes

$$Z(t) = \frac{1}{3\rho}(2\pi)^{-3} \int F_s(k,t) \frac{1}{k^2} \big[C_l(k,t) + 2C_t(k,t) \big] \mathrm{d}\mathbf{k} \tag{9.5.9}$$

If the time correlation functions on the right-hand side of (9.5.9) are replaced by the corresponding hydrodynamic expressions, (9.5.9) leads back to (8.7.15), which is valid for long times. At short times, however, (9.5.9) breaks down: as $t \to 0, Z(t)$ diverges, since $F_s(k, t = 0) = 1$ and $C_l(k, t = 0) = C_t(k, t = 0) = k^2(k_\mathrm{B}T/m)$. To overcome this difficulty a cut-off at large wavenumbers must be introduced in the integration over $\mathbf{k}$. Such a cut-off occurs naturally in the so-called velocity-field approach,[15] in which a result very similar to (9.5.9) is obtained on the basis of a microscopic expression for the local velocity of the tagged particle. This expression involves a 'form factor' $f(r)$, which in the simplest model used is represented by a unit step function that vanishes for distances greater than the particle 'radius' a and has the effect of making the velocity field constant over the range $r \leq a$. Replacement of the Fourier components of the velocity field by their projections along the particle current leads to an expression of the form

$$Z(t) = \frac{1}{3}(2\pi)^{-3} \int \hat{f}(k) F_s(k,t) \frac{1}{k^2} [C_l(k,t) + 2C_t(k,t)] \, \mathrm{d}\mathbf{k} \tag{9.5.10}$$

where $\hat{f}(k = 0) = 1/\rho$ and $\lim_{k\to\infty} \hat{f}(k) = 0$. This result reduces to that obtained by the mode coupling approach in the long-wavelength limit but the behaviour at short times is much improved compared with (9.5.9). In particular, the zero-time value is now correct:

$$Z(0) = (2\pi)^{-3} \int \hat{f}(k) \frac{k_\mathrm{B}T}{m} \, \mathrm{d}\mathbf{k} = \frac{k_\mathrm{B}T}{m} f(r = 0) = \frac{k_\mathrm{B}T}{m} \tag{9.5.11}$$

Equation (9.5.10) does not represent a complete theory, since its evaluation requires a knowledge of the intermediate scattering function and the two current correlation functions. For numerical purposes, however, use can be made of the viscoelastic approximations for $C_l(k,t)$ and $C_t(k,t)$ and the Gaussian approximation (8.2.14) for $F_s(k,t)$. As Figures 9.9 and 9.10 show, results obtained in this way for the velocity autocorrelation function and corresponding

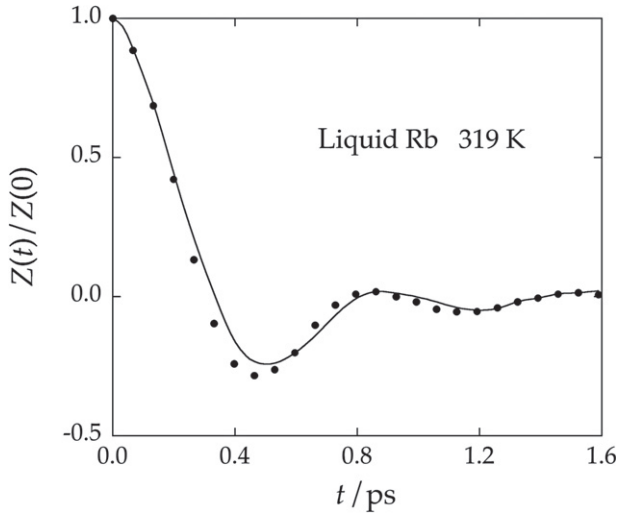

FIGURE 9.9 Normalised velocity autocorrelation function for a model of liquid rubidium. The points are molecular dynamics results and the curve is calculated from the velocity field approximation (9.5.10). From T. Gaskell and S. Miller, 'Longitudinal modes, transverse modes and velocity correlations in liquids: I', *J. Phys. C* **11**, 3749–3761 (1978). © *IOP Publishing 1978. Reproduced by permission of IOP Publishing. All rights reserved.*

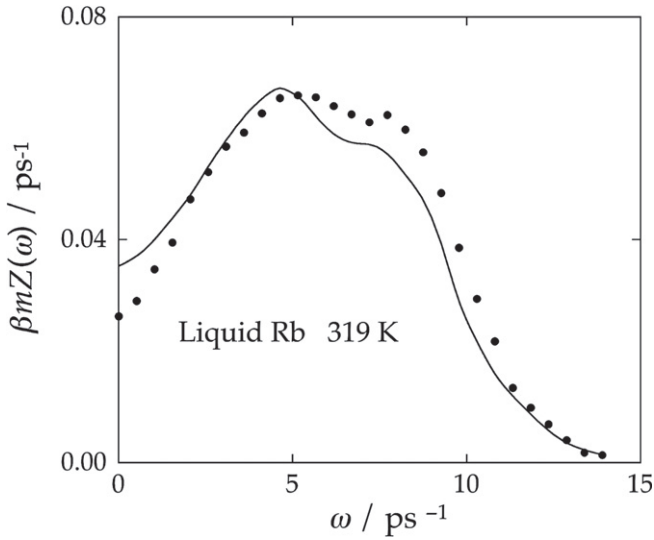

FIGURE 9.10 The power spectrum corresponding to the autocorrelation function plotted in Figure 9.9. The points are molecular dynamics results and the curve is calculated from the velocity field approximation (9.5.10). From T. Gaskell and S. Miller, 'Longitudinal modes, transverse modes and velocity correlations in liquids: I', *J. Phys. C* **11**, 3749–3761 (1978). © *IOP Publishing 1978. Reproduced by permission of IOP Publishing. All rights reserved.*

power spectrum of liquid rubidium are in good agreement with those obtained by molecular dynamics. The pronounced, low-frequency peak in the power spectrum arises from the coupling to the transverse current and the shoulder at higher frequencies comes from the coupling to the longitudinal current.

Another method whereby the short-time behaviour of the mode coupling approximation can be improved is to include the exact, low-order frequency moments of $Z(\omega)$ in a systematic way by working in the continued-fraction representation.[16] Truncation of (9.1.37) at second order gives

$$\tilde{Z}(z) = \cfrac{1}{-iz + \cfrac{\Omega_0^2}{-iz + \tilde{N}_2(z)}} \tag{9.5.12}$$

where Ω_0 is the Einstein frequency (7.2.13) and $\tilde{N}_2(z) \equiv \Delta_2^2 \tilde{M}_2(z)$. The Laplace transform of $\tilde{N}_2(z)$ is related to the autocorrelation function of the second-order random force $R_2 = \mathcal{Q}_2(i\mathcal{L})^2 u_{ix} = \mathcal{Q}_1(i\mathcal{L})^2 u_{ix}$ by

$$\begin{aligned} N_2(t) &= \big(R_2, \exp(i\mathcal{Q}_2\mathcal{L}\mathcal{Q}_2 t)R_2\big)(R_1, R_1\big)^{-1} \\ &= \frac{m}{\Omega_0^2 k_\mathrm{B} T}\big(\mathcal{Q}_1\mathcal{L}^2 u_{ix}, \exp(i\mathcal{Q}_2\mathcal{L}\mathcal{Q}_2 t)\mathcal{Q}_1\mathcal{L}^2 u_{ix}\big) \end{aligned} \tag{9.5.13}$$

The operator $\mathcal{Q}_1 = 1 - \mathcal{P}_1$ projects onto the subspace orthogonal to u_{ix} while $\mathcal{Q}_2 = \mathcal{Q}_1 - \mathcal{P}_2$ projects onto the subspace orthogonal to both u_{ix} and the acceleration $\dot{u}_{ix} = i\mathcal{L}u_{ix}$. The fact that $(i\mathcal{L})^2 u_{ix}$ is automatically orthogonal to $(i\mathcal{L})u_{ix}$ makes it possible to replace $\mathcal{Q}_2$ by $\mathcal{Q}_1$ in the definition of R_2.

If the product variables $\rho_{\mathbf{k}i}\mathbf{j}_{-\mathbf{k}}$ are again chosen as the basis set, use of the approximation (9.5.2) allows (9.5.13) to be rewritten as

$$\begin{aligned} N_2(t) \approx \frac{m}{\Omega_0^2 k_\mathrm{B} T} \sum_{\mathbf{k},\mathbf{k}'} \sum_\alpha \sum_\beta & \big(\rho_{\mathbf{k}'i} j^\beta_{-\mathbf{k}'}, \mathcal{Q}_1\mathcal{L}^2 u_{ix}\big)\big(\rho_{\mathbf{k}'i} j^\beta_{-\mathbf{k}'}, \rho_{\mathbf{k}'i} j^\beta_{-\mathbf{k}'}\big)^{-1} \\ &\times \big(\rho_{\mathbf{k}i} j^\alpha_{-\mathbf{k}}, \exp(i\mathcal{Q}_2\mathcal{L}\mathcal{Q}_2 t)\rho_{\mathbf{k}'i} j^\beta_{-\mathbf{k}'}\big) \\ &\times \big(\rho_{\mathbf{k}i} j^\alpha_{-\mathbf{k}}, \rho_{\mathbf{k}i} j^\alpha_{-\mathbf{k}}\big)^{-1}\big(\mathcal{Q}_1\mathcal{L}^2 u_{ix}, \rho_{\mathbf{k}i} j^\alpha_{-\mathbf{k}}\big) \end{aligned} \tag{9.5.14}$$

If we again assume that the variables $\rho_{\mathbf{k}i}$ and $\mathbf{j}^\alpha_{\mathbf{k}}$ evolve in time independently of each other, and make the further approximation of replacing the projected operator $\mathcal{Q}_2\mathcal{L}\mathcal{Q}_2$ by the full Liouville operator $\mathcal{L}$ in the propagator governing the time evolution of the factorised correlation functions, (9.5.14) becomes

$$\begin{aligned} N_2(t) \approx \frac{m}{\Omega_0^2 k_\mathrm{B} T} \sum_{\mathbf{k},\mathbf{k}'} \sum_\alpha \sum_\beta & \big(\rho_{\mathbf{k}'i} j^\beta_{-\mathbf{k}'}, \mathcal{Q}_1\mathcal{L}^2 u_{ix}\big)\big(\rho_{\mathbf{k}'i} j^\beta_{-\mathbf{k}'}, \rho_{\mathbf{k}'i} j^\beta_{-\mathbf{k}'}\big)^{-1} \\ &\times \big(\rho_{\mathbf{k}i}, \rho_{\mathbf{k}'i}(t)\big)\big(j^\alpha_{-\mathbf{k}}, j^\beta_{-\mathbf{k}'}(t)\big)\delta_{\mathbf{k}\mathbf{k}'} \\ &\times \big(\rho_{\mathbf{k}i} j^\alpha_{-\mathbf{k}}, \rho_{\mathbf{k}i} j^\alpha_{-\mathbf{k}}\big)^{-1}\big(\mathcal{Q}_1\mathcal{L}^2 u_{ix}, \rho_{\mathbf{k}i} j^\alpha_{-\mathbf{k}}\big) \end{aligned} \tag{9.5.15}$$

The time correlation functions appearing here are the same as in (9.5.7), but the time-independent vertices have a more complicated form; a detailed calculation shows that

$$(\mathcal{Q}_1\mathcal{L}^2 u_{i\alpha}, \rho_{\mathbf{k}i} j^{\beta}_{-\mathbf{k}}) = -\frac{\Omega_0^2 k_B T}{m}\mathcal{V}_{\alpha\beta}(k) \tag{9.5.16}$$

where

$$\mathcal{V}_{\alpha\beta}(k) = \frac{\rho}{\Omega_0^2 m}\int \exp(-i\mathbf{k}\cdot\mathbf{r})g(r)\nabla_\alpha\nabla_\beta\, v(r)\,\mathrm{d}\mathbf{r} \tag{9.5.17}$$

is a normalised 'vertex function'. Then, proceeding as before by switching from a sum over wavevectors to an integral, we find that

$$N_2(t) = N_{2l}(t) + 2N_{2t}(t) \tag{9.5.18}$$

with

$$N_{2l,2t}(t) = \frac{\Omega_0^2 m}{3\rho k_B T}(2\pi)^{-3}\int \mathcal{V}^2_{l,t}(k)F_s(k,t)\frac{1}{k^2}C_{l,t}(k,t)\,\mathrm{d}\mathbf{k} \tag{9.5.19}$$

where $\mathcal{V}_{l,t}$ are the longitudinal and transverse components of the vertex tensor, defined in a manner analogous to (7.4.24).

There is a striking similarity between the structure of (9.5.19) and that of the mode coupling expression (9.5.9) obtained earlier for $Z(t)$ except that (9.5.19) contains the vertex factors $\mathcal{V}_{l,t}$. Inclusion of these factors ensures that the integral over wavevectors converges for all t; they therefore play a similar role to that of the form factor $\hat{f}(k)$ in the velocity-field approach, but have the advantage of being defined unambiguously through (9.5.17). The theory is also self-consistent, since the correlation functions required as input may be obtained by a mode coupling calculation of the same type. Numerically, however, the results are less satisfactory than those pictured in Figures 9.9 and 9.10.

9.6 MODE COUPLING THEORY II. THE KINETIC GLASS TRANSITION

The mode coupling ideas introduced in Section 9.5 were first used by Kawasaki[17] to study the 'critical slowing down' of density fluctuations near the liquid-gas critical point. Here we describe the application of the same general approach[18] to the not dissimilar phenomena associated with the kinetic glass transition of a fragile glass former already discussed in a qualitative way in Section 8.8. The theory shows that the structural arrest and associated dynamical anomalies that appear in the supercooled liquid at a well-defined temperature (on cooling) or density (on compression) are a direct consequence of a non-linear, feedback mechanism, the source of which is the fact that the memory function of the density autocorrelation function $F(k,t)$ may be expressed, at least approximately, in terms of $F(k,t)$ itself. Although real glass-forming

liquids are usually multi-component in nature, we limit the discussion to one-component systems; the generalisation to mixtures is straightforward.

We saw in Section 9.4 that the decay of density fluctuations in a simple liquid above its triple point is well described within the memory function formalism by choosing as components of the dynamical vector $\mathbf{A}$ the three variables $\rho_{\mathbf{k}}$ (particle density), $j_{\mathbf{k}} \equiv \mathbf{k}\cdot\mathbf{j}_{\mathbf{k}}/k$ (longitudinal particle current) and $T_{\mathbf{k}}$ (a microscopic temperature variable). It turns out, however, that temperature fluctuations are not important for the description of structural arrest and for present purposes the variable $T_{\mathbf{k}}$ can therefore be omitted. To simplify the resulting equations we first introduce a normalised density autocorrelation function

$$\phi(k,t) = F(k,t)/S(k) \tag{9.6.1}$$

with $\phi(k,t=0)=1$. Then, by following steps similar to those used to derive the memory function equation (9.4.16), we arrive at an expression for the Laplace transform of $\phi(k,t)$ in the form

$$\tilde{\phi}(k,z) = \frac{1}{-iz + \dfrac{\Omega_k^2}{-iz + \tilde{M}(k,z)}} \tag{9.6.2}$$

where $\Omega_k^2 = v_T^2 k^2/S(k)$ and $v_T = (k_{\mathrm{B}}T/m)^{1/2}$ is the thermal velocity. The structure of this result is identical with that in (9.4.16) and the function $\tilde{M}(k,z)$, like $\tilde{N}_l(k,z)$ in (9.4.16), is again the memory function of the longitudinal current, but the choices made for the vector $\mathbf{A}$ means that the explicit form of the memory function is different in the two cases. In the two-variable description the random-force vector has only one component, given by

$$K_{\mathbf{k}} = \mathcal{Q}(i\mathcal{L}j_{\mathbf{k}}) \tag{9.6.3}$$

and the corresponding memory function is

$$M(k,t) = \frac{1}{Nv_T^2}\big(K_{\mathbf{k}}, R_{\mathbf{k}}(t)\big) \tag{9.6.4}$$

with $R_{\mathbf{k}}(t) = \exp(i\mathcal{Q}\mathcal{L}\mathcal{Q}t)K_{\mathbf{k}}$, where the operator $\mathcal{Q} = 1-\mathcal{P}$ projects an arbitrary dynamical variable onto the subspace orthogonal to the variables $\rho_{\mathbf{k}}$ and $j_{\mathbf{k}}$. The time dependence of $\phi(k,t)$ is obtained from (9.6.2) via an inverse Laplace transform:

$$\ddot{\phi}(k,t) + \Omega_k^2\phi(k,t) + \int_0^t M(k,t-t')\dot{\phi}(k,t')\,\mathrm{d}t' \tag{9.6.5}$$

which can be recognised as the equation of motion of a harmonic oscillator of frequency Ω_k, damped by a time-retarded, frictional force.

The theoretical task is to derive an expression for the memory function that accounts for the structural slowing down near the transition temperature T_{C}; to achieve this, we follow the original arguments of Götze and collaborators.[19]

The random force $K_{\mathbf{k}}$ is by construction orthogonal to the slow variable $\rho_{\mathbf{k}}$ and the simplest slow variables having a non-zero correlation with $K_{\mathbf{k}}$ are the pair products

$$A_{\mathbf{p},\mathbf{q}} = \rho_{\mathbf{p}}\rho_{\mathbf{q}} \tag{9.6.6}$$

Hence the first approximation, one of typical mode coupling type, is to replace the random force $K_{\mathbf{k}}$ in (9.6.3) by its projection onto the subspace spanned by all pair products, i.e.

$$K_{\mathbf{k}} \approx \sum_{\mathbf{p},\mathbf{q}} \sum_{\mathbf{p}',\mathbf{q}'} (A_{\mathbf{p}',\mathbf{q}'}, K_{\mathbf{k}})(A_{\mathbf{p},\mathbf{q}}, A_{\mathbf{p}',\mathbf{q}'})^{-1} A_{\mathbf{p},\mathbf{q}} \tag{9.6.7}$$

Substitution of (9.6.7) and the corresponding expression for $R_{\mathbf{k}}(t)$ in (9.6.4) gives

$$\begin{aligned} M(k,t) = \frac{1}{N v_T^2} &\sum_{\mathbf{p},\mathbf{q}} \sum_{\mathbf{p}',\mathbf{q}'} (A_{\mathbf{p}',\mathbf{q}'}, K_{\mathbf{k}})(A_{\mathbf{p},\mathbf{q}}, A_{\mathbf{p}',\mathbf{q}'})^{-1} \\ &\times \sum_{\mathbf{p}'',\mathbf{q}''} \sum_{\mathbf{p}''',\mathbf{q}'''} (A_{\mathbf{p}''',\mathbf{q}'''}, K_{\mathbf{k}})(A_{\mathbf{p}'',\mathbf{q}''}, A_{\mathbf{p}''',\mathbf{q}'''})^{-1} \\ &\times \left(A_{\mathbf{p},\mathbf{q}}, \exp(i\mathcal{Q}\mathcal{L}\mathcal{Q}t) A_{\mathbf{p}'',\mathbf{q}''}\right) \end{aligned} \tag{9.6.8}$$

The next step is to factorise the static and dynamic four-point correlation functions in (9.6.8) into products of two-point functions, and simultaneously to replace the propagator of the projected dynamics by the full propagator. Thus

$$\begin{aligned} \left(A_{\mathbf{p},\mathbf{q}}, \exp(i\mathcal{Q}\mathcal{L}\mathcal{Q}t) A_{\mathbf{p}'',\mathbf{q}''}\right) &= \left(\rho_{\mathbf{p}}\rho_{\mathbf{q}}, \exp(i\mathcal{Q}\mathcal{L}\mathcal{Q}t)\rho_{\mathbf{p}''}\rho_{\mathbf{q}''}\right) \\ &\approx \left(\rho_{\mathbf{p}}, \exp(i\mathcal{L}t)\rho_{\mathbf{p}''}\right)\left(\rho_{\mathbf{q}}, \exp(i\mathcal{L}t)\rho_{\mathbf{q}''}\right) \\ &= \delta_{\mathbf{p},\mathbf{p}''}\delta_{\mathbf{q},\mathbf{q}''} N^2 S(p) S(q) \phi(p,t)\phi(q,t) \end{aligned} \tag{9.6.9}$$

while for $t = 0$:

$$(A_{\mathbf{p},\mathbf{q}}, A_{\mathbf{p}',\mathbf{q}'})^{-1} = \frac{\delta_{\mathbf{p},\mathbf{p}'}\delta_{\mathbf{q},\mathbf{q}'}}{N^2 S(p) S(q)} \tag{9.6.10}$$

The three-point static correlation functions that appear in the terms involving $K_{\mathbf{k}}$ in (9.6.8) can be eliminated with a help of a generalisation of the Yvon equality (7.2.11), i.e.

$$\left\langle \dot{A} B^* \right\rangle = \left\langle (i\mathcal{L}A) B^* \right\rangle \equiv -\left\langle \{\mathcal{H}, A\} B^* \right\rangle = k_B T \left\langle \{A, B^*\} \right\rangle \tag{9.6.11}$$

the proof of which now requires a double integration by parts. We also make use of the Ornstein–Zernike relation in the form $S(k) = 1/(1 - \rho\hat{c}(k))$ and the convolution approximation (4.2.10). Then, for example:

$$(\rho_{\mathbf{p}',\mathbf{q}'}, i\mathcal{L}j_{\mathbf{k}}) = -\frac{i v_{\mathrm{T}}^2 N \delta_{\mathbf{k},\mathbf{p}'+\mathbf{q}'}}{k} \left[\mathbf{k}\cdot\mathbf{p}' S(q') + \mathbf{k}\cdot\mathbf{q}' S(p')\right] \tag{9.6.12}$$

The final result of these manipulations is

$$M(k,t) = \frac{v_T^2 \rho^2}{2Nk^2} \sum_{\mathbf{p},\mathbf{q}} \delta_{\mathbf{k},\mathbf{p}+\mathbf{q}} S(p)S(q)\left[\hat{c}(p)\mathbf{k}\cdot\mathbf{p} + \hat{c}(q)\mathbf{k}\cdot\mathbf{q}\right]^2 \phi(p,t)\phi(q,t) \tag{9.6.13}$$

The factor $\frac{1}{2}$ on the right-hand side arises from the fact that all double sums over pairs of wavevectors must be ordered in such a way that each product variable $A_{\mathbf{p},\mathbf{q}}$ appears only once.

The appearance of the product $\phi(p,t)\phi(q,t)$ in (9.6.13) means that the memory function decays on the same timescale as the correlation function. This represents only the long-time contribution to the total memory function and cannot describe the behaviour at short times, which is dominated by nearly instantaneous, binary collisions. To describe the effect of collisions it is assumed that the short-time contribution $M^{(0)}(k,t)$ can be represented by a δ-function, i.e.

$$M^{(0)}(k,t) = \nu(k)\delta(t) \tag{9.6.14}$$

The complete memory function is therefore written as

$$M(k,t) = \nu(k)\delta(t) + \Omega_k^2 m(k,t) \tag{9.6.15}$$

Comparison with (9.6.13) shows that

$$m(k,t) = \frac{1}{2V} \sum_{\mathbf{p},\mathbf{q}} \delta_{\mathbf{k},\mathbf{p}+\mathbf{q}} \mathcal{V}(\mathbf{k},\mathbf{p},\mathbf{q})\phi(p,t)\phi(q,t) \tag{9.6.16}$$

where the vertex function $\mathcal{V}$ is

$$\mathcal{V}(\mathbf{k},\mathbf{p},\mathbf{q}) = \frac{\rho}{k^4} S(k)S(p)S(q)\left[\hat{c}(p)\mathbf{k}\cdot\mathbf{p} + \hat{c}(q)\mathbf{k}\cdot\mathbf{q}\right]^2 \tag{9.6.17}$$

The non-linear, integro-differential equation (9.6.5) may then be rewritten as

$$\ddot{\phi}(k,t) + \Omega_k^2\phi(k,t) + \nu(k)\dot{\phi}(k,t) + \Omega_k^2 \int_0^\infty m(k,t-t')\dot{\phi}(k,t')\mathrm{d}t' = 0 \tag{9.6.18}$$

The coupled equations (9.6.16) and (9.6.18) form a closed, self-consistent set; the only input required for their solution is the static structure factor of the supercooled liquid, which determines the value of the vertex function via (9.6.17). The feedback mechanism is provided by the quadratic dependence of the memory function on $\phi(k,t)$, with the density and temperature dependence of the effect coming from the vertex function. Numerical solution of the coupled equations reveals the existence of a sharp crossover from ergodic to non-ergodic behaviour of $\phi(k,t)$ at a well-defined temperature (at constant density) or density (at constant temperature). The predicted correlation function can also be used as input to a similar set of equations for the self-correlation function $F_s(k,t)$, where the memory function now involves the product $\phi(k,t)F_s(k,t)$.

In the case of hard spheres the theory outlined above predicts a kinetic glass transition at a packing fraction $\eta_C \approx 0.516$ when the Percus–Yevick approximation for the structure factor is used. At the critical packing fraction the order parameter[20] $f_k = \lim_{t\to\infty} \phi(k,t)$ changes discontinuously from zero to a wavenumber-dependent value $0 < f_k \leq 1$. That this transition is a direct consequence of the non-linearity of the equation of motion (9.6.18) can be demonstrated with the help of some further approximations.[19,21] The largest contribution to the vertex function comes from the region $k \approx k_{\max}$ of the main peak in the structure factor. It is therefore not unreasonable to ignore the sum over wavevectors by putting $S(k) \approx 1 + a\delta(k - k_{\max})$, where a is the area under the main peak. With this assumption, (9.6.18) becomes an equation for the single correlation function $\phi(k_{\max}, t) \equiv \phi(t)$, which we write as

$$\ddot{\phi}(t) + \Omega^2\phi(t) + \nu\dot{\phi}(t) + \lambda\Omega^2 \int_0^\infty [\phi(t-t')]^2\dot{\phi}(t')\,\mathrm{d}t' = 0 \qquad (9.6.19)$$

where $\Omega \equiv \Omega_{k_{\max}}$, ν can be interpreted as a collision frequency and λ, which replaces the complicated vertex function, acts as a 'control parameter', a role played by inverse temperature or density in the more complete theory. By taking the Laplace transform of (9.6.19) we recover (9.6.2) in the form

$$\tilde{\phi}(z) = \cfrac{1}{-iz + \cfrac{\Omega^2}{-iz + \nu + \Omega^2\tilde{m}(z)}} \qquad (9.6.20)$$

with

$$\tilde{m}(z) = \lambda \int_0^\infty [\phi(t)]^2 \exp(izt)\mathrm{d}t \qquad (9.6.21)$$

Equation (9.6.20) can be rearranged to give

$$\frac{\tilde{\phi}(z)}{1 + iz\tilde{\phi}(z)} = \frac{1}{\Omega^2}\big[-iz + \nu + \Omega^2\tilde{m}(z)\big] \qquad (9.6.22)$$

Let $\lim_{t\to\infty} \phi(t) = f$, where the order parameter f is now independent of k. Then

$$\lim_{z\to 0} \tilde{\phi}(z) = \frac{f}{-iz} \qquad (9.6.23)$$

and hence, from substitution in (9.6.22):

$$\lim_{z\to 0} \tilde{m}(z) = \frac{f}{-iz(1-f)} \qquad (9.6.24)$$

In the non-ergodic or structurally arrested phase, where $f > 0$, the power spectrum $\phi(\omega)$ will contain a fully elastic component, $f\delta(\omega)$; experimentally this would correspond to scattering from the frozen structure.

Equation (9.6.21) shows that

$$\lim_{z\to 0} \tilde{m}(z) = \frac{\lambda f^2}{-iz} \qquad (9.6.25)$$

Identification of (9.6.25) with (9.6.24) leads to a simple equation for the order parameter:

$$\frac{f}{1-f} = \lambda f^2 \tag{9.6.26}$$

the solutions to which are

$$f = 0, \quad f = \frac{1}{2}\left[1 \pm (1 - 4/\lambda)^{1/2}\right] \tag{9.6.27}$$

Since f must be real, the only acceptable solution for $\lambda < 4$ is $f = 0$, corresponding to the ergodic phase. This remains a solution at larger values of λ, but at the critical value, $\lambda_C = 4$, there is a bifurcation to the non-ergodic solution, $f = \frac{1}{2}[1+(1-4/\lambda)^{1/2}]$; for $\lambda = 4$, $f = \frac{1}{2}$. The root $f = \frac{1}{2}[1-(1-4/\lambda)^{1/2}]$ is not acceptable, since it implies that the system would revert to ergodic behaviour in the limit $\lambda \to \infty$. Let $\lambda = 4(1 + \sigma\epsilon)$, where $\sigma = -1$ and $+1$ in the ergodic and arrested phases, respectively. The quantity $\epsilon = (\lambda - \lambda_C)/\sigma\lambda_C$ is a positive number which measures the distance from the transition. Substitution in (9.6.27) shows that for $\sigma = +1$, f has a square-root cusp as $\epsilon \to 0$:

$$\lim_{\epsilon \to 0} f = \frac{1}{2}\left(1 + \epsilon^{1/2}\right) \tag{9.6.28}$$

The dependence of f on λ calculated from (9.6.27) and (9.6.28) is sketched in Figure 9.11.

Equation (9.6.28) describes the infinite-time behaviour of the correlation function in the arrested phase for $\lambda \approx \lambda_C$. To extend this result to finite times,

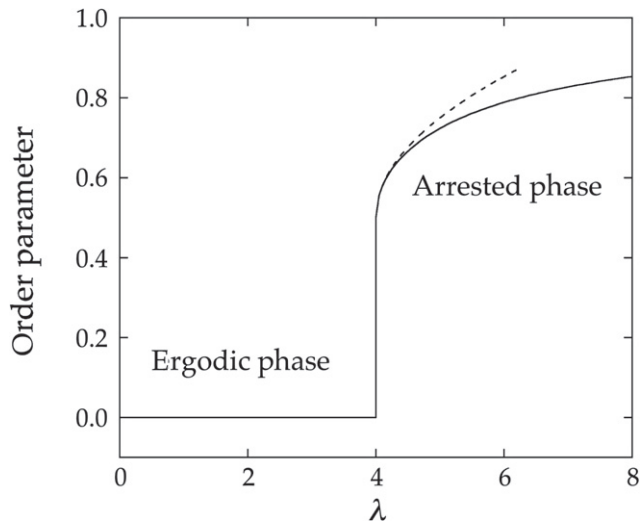

FIGURE 9.11 Predictions of mode coupling theory for the dependence on λ of the order parameter f. The full curve is the result obtained from the equation of motion (9.6.19) and the dashes show the approximate solution (9.6.27).

we look for a solution to (9.6.19) of the form

$$\phi(t) = \frac{1}{2} + \epsilon^{1/2} g_\epsilon(\tau) \tag{9.6.29}$$

where $\tau = \epsilon^s t$ is a scaled time and $g_\epsilon(\tau)$ is a scaling function. The quantity $s(>0)$ is a scaling exponent, which is determined later by requiring $\phi(t)$ to be independent of ϵ in the short-time limit. This restriction on ϕ follows from the fact that the short-time behaviour is controlled by the collision frequency ν, not by the mode coupling contribution to the memory function. The Laplace transform of (9.6.29) is

$$\tilde{\phi}(z) = \epsilon^{-s}\left(\frac{1}{-2i\zeta} + \epsilon^{1/2}\tilde{g}_\epsilon(\zeta)\right) \tag{9.6.30}$$

where $\zeta \equiv \epsilon^{-s} z$. If we substitute (9.6.29) in (9.6.21) (with $\lambda = 4 + 4\sigma\epsilon$) and (9.6.30) in (9.6.22), combine the two results and let $\epsilon \to 0$, we obtain an equation for the scaling function at the critical point ($\epsilon = 0$):

$$-8i\zeta[\tilde{g}_0(\zeta)]^2 - 4\int_0^\infty [g_0(\tau)]^2 \exp(i\zeta\tau)\mathrm{d}\tau = \frac{\sigma}{-i\zeta} \tag{9.6.31}$$

To derive this result it must be assumed that $\epsilon^{1/2}\tilde{g}_0(\zeta)$ vanishes with ϵ; the solution obtained below is consistent with that assumption.

The β-relaxation regime corresponds to scaled times $\tau \ll 1$ (or $\zeta \gg 1$). We look for a power-law solution for $g_0(\tau)$ such that

$$g_0(\tau) = a_0\tau^{-a}, \quad \tau \to 0 \tag{9.6.32}$$

with a Laplace transform given by

$$\tilde{g}_0(\zeta) = a_0\Gamma(1-a)(-i\zeta)^{a-1}, \quad \zeta \to \infty \tag{9.6.33}$$

where $\Gamma(x)$ is the gamma function. Substitution in (9.6.31) gives

$$(-i\zeta)^{2a-1}4a_0^2\left[2\Gamma^2(1-a) - \Gamma(1-2a)\right] = 0 \tag{9.6.34}$$

i.e. $2\Gamma^2(1-a) = \Gamma(1-2a)$, the positive solution to which is $a \approx 0.395$. When written in terms of the original time variable t, combination of (9.6.29) and (9.6.32) shows that

$$\phi(t) = \frac{1}{2} + a_0\epsilon^{-as+1/2}t^{-a} \tag{9.6.35}$$

Since $\phi(t)$ must be independent of ϵ in the limit $t \to 0$, it follows that $s = 1/2a \approx 1.265$. Thus the correlation function decays as

$$\phi(t) = \frac{1}{2} + a_0 t^{-a} \tag{9.6.36}$$

The result expressed by (9.6.36) is independent of σ. It therefore describes both the decay of $\phi(t)$ towards its non-zero, asymptotic value in the arrested phase and the first relaxation process in the ergodic phase, where the power-law behaviour will persist so long as $\tau \ll 1$. Times $\tau \gg 1$ correspond to α-relaxation in the ergodic phase. A scaling analysis similar to the previous

one starts from the ansatz

$$g_0(\tau) = -b_0\tau^b, \quad \tau \to \infty \tag{9.6.37}$$

and leads to the exponent relation

$$2\Gamma^2(1+b) - \Gamma(1+2b) = 0 \tag{9.6.38}$$

The only acceptable solution to this equation is $b = 1$. Thus

$$\phi(t) = \frac{1}{2} - b_0\epsilon^{1/2}\tau, \quad 1 \ll \tau \ll 1/b_0\epsilon^{1/2} \tag{9.6.39}$$

The upper limit on τ in (9.6.39) appears because $|\epsilon^{1/2}g_0(\tau)|$ must be less than unity for the asymptotic analysis to be valid. At yet longer times a purely exponential decay is predicted, in contrast to the stretched exponential decay seen both experimentally and in simulations (see Section 8.8). To reproduce the observed behaviour the simplified model represented by (9.6.19), in which $m(t)$ behaves as $[\phi(t)]^2$, must be generalised[18] to include more control parameters and other powers of $\phi(t)$.

The scaling predictions of mode coupling theory have been tested against experimental data and the results of simulations, and generally good agreement is found at temperatures just above T_C. However, the distinction between ergodic and strictly non-ergodic phases that appears in the original version of the theory is unrealistic. At sufficiently long times thermally activated processes of the type evident, for example, in Figure 8.11 will eventually cause ergodicity to be restored. Such effects can be accommodated within the theory by inclusion of the coupling of fluctuations in the microscopic density with those in particle current.[22] The 'ideal' transition is then suppressed and the correlation function is found to decay to zero even below T_C, though only after a period of near-complete structural arrest that rapidly lengthens as the temperature is lowered.

Mode coupling theory has also been extended to the case of concentrated, colloidal solutions. As we shall see in Chapter 12, these are systems that are well described by potentials consisting of a hard-core repulsion and a very short-ranged attractive interaction which favours aggregation of particles. Higher-order glass transition singularities are predicted, resulting in a re-entrant, liquid–glass transition line in the temperature–density plane and a transition line between two glass states.[23] Another generalisation of the theory deals with inhomogeneous, supercooled liquids,[24] and is therefore relevant to the phenomenon of dynamical heterogeneity discussed in Section 8.8.[25]

REFERENCES

[1] Zwanzig, R., *In* 'Lectures in Theoretical Physics', vol. III (W.E. Britton, B.W. Downs and J. Downs, eds). Wiley Interscience, New York, 1961.

[2] (a) Mori, H., *Prog. Theor. Phys.* **33**, 423 (1965). (b) Mori, H., *Prog. Theor. Phys.* **34**, 399 (1965).

[3] Lovesey, S.W., *J. Phys. C* **6**, 1856 (1973).
[4] See, e.g., de Jong, P.H.K., Verkerk, P. and de Graaf, L.A., *J. Phys.: Cond. Matter* **6**, 8391 (1994).
[5] Balucani, U., Torcini, A., Stangl, A. and Morkel, C., *J. Non-Cryst. Solids* **205–207**, 299 (1996).
[6] Levesque, D. and Verlet, L., *Phys. Rev. A* **2**, 2514 (1970).
[7] Levesque, D., Verlet, L. and Kürkijarvi, J., *Phys. Rev. A* **7**, 1690 (1973).
[8] See, e.g., Kambayashi, S. and Kahl, G., *Phys. Rev. A* **46**, 3255 (1992).
[9] Lovesey, S.W., *J. Phys. C* **4**, 3057 (1971).
[10] Rahman, A., *In* 'Statistical Mechanics: New Concepts, New Problems, New Applications' (S.A. Rice, K.F. Freed and J.C. Light, eds). University of Chicago Press, Chicago, 1972.
[11] Copley, J.R.D. and Lovesey, S.W., *Rep. Prog. Phys.* **38**, 461 (1975).
[12] Values of $\tau_1(k)$ obtained from separate fits of $C_t(k,\omega)$ and $S(k,\omega)$ are nearly the same; the small differences that do occur can be ascribed to statistical uncertainties in the molecular dynamics data.
[13] (a) Scopigno, T., Balucani, U., Ruocco, G. and Sette, F., *Phys. Rev. Lett.* **85**, 4076 (2000). (b) Scopigno, T., Balucani, U., Ruocco, G. and Sette, F., *J. Non-Cryst. Solids* **312–314**, 121 (2002).
[14] See Monaco, A., Scopigno, T., Benassi, P., Giugni, A., Monaco, G., Nardone, M., Ruocco, G. and Sampoli, M., *J. Chem. Phys.* **120**, 8089 (2004) (for K) and references therein to work on Na, Al and Ga.
[15] Gaskell, T. and Miller, S., *J. Phys. C* **11**, 3749 (1978).
[16] Bosse, J., Götze, W. and Zippelius, A., *Phys. Rev. A* **18**, 1214 (1978).
[17] Kawasaki, K., *Ann. Phys. NY* **61**, 1 (1970).
[18] (a) Götze, W. and Sjögren, L., *Rep. Prog. Phys.* **55**, 241 (1992). (b) Götze, W., *In* 'Liquids, Freezing and the Glass Transition: Les Houches, Session LI' (J.P. Hansen, D. Levesque and J. Zinn-Justin, eds). Elsevier, Amsterdam, 1991. (c) Das, S.P., *Rev. Mod. Phys.* **76**, 785 (2004).
[19] Bengtzelius, U., Götze, W. and Sjölander, A., *J. Phys. C* **17**, 5915 (1984).
[20] The terms non-ergodicity parameter or Edwards–Anderson parameter are also used, the latter by analogy with a related problem in the theory of spin glasses: Edwards, S.F. and Anderson P.W., *J. Phys. F* **5**, 965 (1975).
[21] Leutheusser, E., *Phys. Rev. A* **29**, 2765 (1984).
[22] (a) Das, S.P. and Mazenko, G.F., *Phys. Rev. A* **34**, 2265 (1986). (b) Götze, W. and Sjögren, L., *Z. Phys. B* **65**, 415 (1987).
[23] Dawson, K., Foffi, G., Fuchs, M., Götze, W., Sciortino, F., Sperl, M., Tartaglia, P., Voigtmann, Th. and Zaccarelli, E., *Phys. Rev. E* **63**, 011401 (2000).
[24] Biroli, G., Bouchaud, J.P., Miyazaki, K. and Reichman, D.R., *Phys. Rev. Lett.* **97**, 195701 (2006).
[25] For a full review of all aspects of dynamical slowing down, see Götze, W., 'Complex Dynamics of Glass-Forming Liquids: A Mode-Coupling Theory'. Oxford University Press, New York, 2009.